# Seasonal Characteristics of New Particle Formation and Growth in Urban Beijing

Deng, Chenjuan

2020-07-21

Deng , C , Fu , Y , Dada , L , Yan , C , Cai , R , Yang , D , Zhou , Y , Yin , R , Lu , Y , Li , X , Qiao , X , Fan , X , Nie , W , Kontkanen , J , Kangasluoma , J , Chu , B , Ding , A , Kerminen , V-M , Paasonen , P , Worsnop , D R , Bianchi , F , Liu , Y , Zheng , J , Wang , L , Kulmala , M & Jiang , J 2020 , ' Seasonal Characteristics of New Particle Formation and Growth in Urban Beijing ' , Environmental Science & Technology , vol. 54 , no. 14 , pp. 8547-8557 . https://doi.org/10.1021/acs.

http://hdl.handle.net/10138/332501
https://doi.org/10.1021/acs.est.0c00808

acceptedVersion

Article Id: es0c00808

| Query Link | Query |
|---|---|
| [1] | Please provide updated publication information for ref 24, if available. |
| [2] | Please provide updated publication information for ref 40, if available. |

# Seasonal ~~characteristics~~Characteristics of ~~new particle formation~~New Particle Formation and ~~growth~~Growth in ~~urban~~Urban Beijing

Chenjuan~~-~~ Deng[†‡], Yueyun~~-~~ Fu[†‡], Lubna~~-~~ Dada[‡‡], Chao~~-~~ Yan[‡‡,§§], Runlong~~-~~ Cai[†‡], Dongsen~~-~~ Yang[∥⊥], Ying~~-~~ Zhou[§§], Rujing~~-~~ Yin[†‡], Yiqun~~-~~ Lu[⊤⊥], Xiaoxiao~~-~~ Li[†‡], Xiaohui~~-~~ Qiao[†‡], Xiaolong~~-~~ Fan[§§], Wei~~-~~ Nie[#], Jenni~~-~~ Kontkanen[‡‡], Juha~~-~~ Kangasluoma[‡‡,§§], Biwu~~-~~ Chu[‡‡,§§], Aijun~~-~~ Ding[#], Veli-Matti~~-~~ Kerminen[‡‡], Pauli~~-~~ Paasonen[‡‡], Douglas R.~~-~~ Worsnop[‡‡,▽▽], Federico~~-~~ Bianchi[‡‡], Yongchun~~-~~ Liu[§§], Jun~~-~~ Zheng[∥⊥], Lin~~-~~ Wang[⊤⊥], Markku~~-~~ Kulmala[*,‡‡,§§], Jingkun~~-~~ Jiang[**,†‡]

[†‡]~~-~~ State Key Joint Laboratory of Environment Simulation and Pollution Control, School of Environment, Tsinghua University, 100084 Beijing, China

[‡‡]~~-~~ Institute for Atmospheric and Earth System ~~Research/Physics,~~ Research Physics, Faculty of Science, University of Helsinki, 00014 Helsinki, Finland

[§§]~~-~~ Aerosol and Haze Laboratory, Beijing Advanced Innovation Center for Soft Matter Science and Engineering, Beijing University of Chemical Technology, 100029 Beijing, China

[∥⊥]~~-~~ Collaborative Innovation Center of Atmospheric Environment and Equipment Technology, Nanjing University of Information Science and Technology, 210044 Nanjing, China

[⊤⊥]~~-~~ Shanghai Key Laboratory of Atmospheric Particle Pollution and Prevention (LAP3), Department of Environmental Science and Engineering, Fudan University, ~~Shanghai~~200433 Shanghai, China

[#]~~-~~ Joint International Research Laboratory of Atmospheric and Earth System Sciences, School of Atmospheric Sciences, Nanjing University, 210023 Nanjing, China

[▽▽]~~-~~ Aerodyne Research Inc., Billerica, Massachusetts 01821, ~~USA~~United States

[*]~~-~~ ~~email:~~Email: markku.kulmala@helsinki.fi.

[**]~~-~~ ~~email:~~Email: jiangjk@tsinghua.edu.cn.

22-06-2020

## Abstract

Understanding the atmospheric new particle formation (NPF) process within the global range is important for revealing the budget of atmospheric aerosols and their impacts. We investigated the seasonal characteristics of NPF in the urban environment of Beijing. Aerosol size distributions down to ~~1~~~1 nm and $H_2SO_4$ concentration were measured during ~~2018–2019.~~2018–2019. The observed formation rate of 1.5 nm particles ($J_{1.5}$) is significantly higher than those in the clean environment, e.g., ~~Hyytiälä;~~Hyytiälä, whereas the growth rate is relatively lower. Both $J_{1.5}$ and NPF frequency in urban Beijing showed a clear seasonal variation with maxima in winter and minima in summer, while the observed growth rates were generally within the same range around the year. We show that ambient temperature is a governing factor driving the seasonal variation of $J_{1.5}$. In contrast, the condensation sink showed no significant seasonal variation during the NPF periods and the daily maximum $H_2SO_4$ concentration was slightly higher in summer than ~~that~~ in winter. In all four seasons, condensation of $H_2SO_4$ and $(H_2SO_4)_{~~n~~n}$(amine)$_{~~n~~n}$ clusters contributes significantly to the growth rates in the sub-3 nm size range, whereas it is less important for the observed growth rates of particles above 3 nm. Therefore, other species are always needed for the growth of larger particles.

## Keywords

~~New Particle Formation~~new particle formation; ~~Growth~~growth; seasonal varia~~Seasonal Variation~~tion; ~~Temperature Influence~~temperature influence

## 1 ~~.~~ . Introduction

TOC ArtPlace Figure 1 HerePlace Figure 2 HerePlace Figure 3 HerePlace Figure 4 HerePlace Figure 5 HerePlace Figure 6 HerePlace Figure 7 Here**Supplementary Information**Corresponding AuthorJingkun JiangMarkku KulmalaAtmospheric new particle formation (NPF) refers to the conversion from gaseous precursors to new particles. It is ubiquitous and contributes majorly to the global aerosol ~~population~~population.[1–3] ~~.~~ Once growing past certain sizes, the newly formed particles can be activated as the cloud condensation nuclei (CCN) ~~and thus~~and, thus, influence cloud formation and global ~~climate~~climate.[4,5] ~~.~~ It is estimated that around half of global CCN in the lower troposphere are derived from atmospheric ~~NPF~~NPF.[5,6] ~~.~~

To understand the NPF phenomenon within the wide global range, many field studies were conducted throughout the world in both pristine and polluted ~~environments~~environments.[1,7,8] ~~.~~ Different from relatively clean environments, the concentration of pre-existing aerosols is high in polluted environments, which suppresses NPF by acting as a sink for both condensable vapors and newly formed particles.[9–11] ~~.~~ Despite the strong suppression by the high aerosol loading in polluted environments, intensive NPF events have still been frequently observed in these ~~environments~~environments.[8,11–15] ~~.~~

Seasonal characteristics of NPF have been explored in urban ~~Beijing~~Beijing.[16,17] ~~.~~ However, due to limitations in applied instruments in these long-term studies, there is practically no information about key precursors for new particle formation (e.g., $H_2SO_4$) and size distributions of sub-3 nm particles. Although the $H_2SO_4$ concentration was measured in two short-term field campaigns in urban Beijing[11,18] and its daily maximum concentration ranged from ~~~10~~~10$^5$ to 1.9 ~~×~~× 10$^7$ cm~~−3~~$^{-3}$, the seasonal variation of the $H_2SO_4$ concentration in Beijing has not yet been reported. ~~Long-term~~ The long-term size distribution data for sub-3 nm particles has also been missing from previous studies in Beijing and even rarely reported in other environments. As shown in a recent ~~study~~study,[19] ~~,~~ previously reported particle formation rates for urban Beijing (inferred from ~~large sized~~ large-sized particles) were underestimated and sub-3 nm particle size distributions (PSDs) are needed to accurately quantify these rates.

When evaluating the particle formation rate from measured data, underestimating coagulation scavenging can lead to significant underestimation of the particle formation rate, especially for polluted environments and controlled chamber studies having a strong coagulation effect. Cai and Jiang[19] found that the ~~commonly-used~~ commonly used formulae underestimate the formation rate of 1.5 nm particles in urban Beijing, so they derived an improved formula with a more accurate treatment of the coagulation effect. Also, due to the underestimation of the coagulation effect, new particle formation rates from ~~CLOUD (Cosmics~~the Cosmics Leaving OUtdoor ~~Droplets)~~ Droplets (CLOUD) chamber studies on sulfuric acid-dimethylamine (DMA) nucleation were later corrected to be a factor of 10 faster than previously published ~~results~~results.[20] ~~.~~ In addition, Cai et al.[21] ~~shows~~showed that neglecting coagulation scavenging can result in overestimation when ~~evaluationg~~ evaluating the particle growth rate from the measured data.

Although clear seasonal variations in the frequency of NPF events ~~has~~have been observed in urban ~~Beijing~~Beijing,[16,17] ~~,~~ the factors governing these seasonal variations ~~remains~~remain to be revealed. The concentrations of gaseous precursors and the coagulation scavenging effect of the pre-existing aerosols are important factors that govern the occurrence and the intensity of NPF. Their synergetic effect on NPF can be evaluated using dimensionless parameters such as $L$[22] or $L_{FT}$.[23] ~~.~~ Using $L_{FT}$, Cai et al.[11] showed that the pre-existing aerosol surface area governs the occurrence of NPF in Beijing in a short-term campaign. In addition to pre-existing aerosols and $H_2SO_4$ concentration, other factors, such as ambient temperature and concentration of base molecules, may also affect NPF. Recently, Cai et al.[24] showed that the NPF events in urban Beijing are dominated by $H_2SO_4$-amine nucleation and proposed a new parameter, $I$, for predicting the occurrence of NPF in environments governed by $H_2SO_4$-amine nucleation. Factors governing the seasonal variation of NPF in urban Beijing can be explored with the help of this new parameter.

In addition to the formation of new particles, the subsequent growth of these particles and ~~its~~their seasonal characteristics are also of great importance. The particle growth rates in the ~~3–25~~3–25 nm size range were reported to be slightly higher in summer than in other seasons in

~~Beijing~~Beijing.[17]~~.~~ However, the seasonal variation of the observed growth rates in different size ranges has not yet been reported in urban Beijing, especially in the sub-3 nm size range. As a condensable vapor, $H_2SO_4$ contributes to the particle growth; however, its contribution usually decreases with an increasing particle ~~size~~size.[25–27]~~.~~ In addition to $H_2SO_4$, small ~~acid-base~~acid–base clusters can also contribute to the particle growth, especially in the sub-3 nm size ~~range~~range.[28]~~.~~

In this study, we report the results of long-term field measurements conducted in urban Beijing during ~~2018–2019,~~2018–2019, including the measurements of particle size distribution down to ~~~~1~~1 nm and $H_2SO_4$ concentration. We focus on seasonal characteristics of new particle formation rates and growth rates and explore factors governing the observed seasonal characteristics. We also compare the characteristics of NPF in urban Beijing with observations in other atmospheric environments.

## 2~~.~~. Methods

### 2.1~~.~~. Measurements

The observation site is located on the top of a five-floor building at Beijing University of Chemical Technology (West Campus), Beijing. The sampling inlets are located ~~~~20~~20 m above the ground and ~~~~150~~150 m to the southwest of a road. The Third Ring Road is ~~~~550~~550 m to the east of the ~~site~~site, and as a major road, the traffic is often busy. More details on the site can be found in the study reported by Lu et al.[29] and Zhou et al.[30]~~.~~ There are no significant stationary emission sources nearby. However, the emission from vehicles may influence the measured aerosols and gaseous pollutants.

The wide-range size distributions of 1 ~~nm - 10 μm~~ nm–10 μm particles were measured using a prototype diethylene glycol scanning mobility particle spectrometer (DEG-SMPS; ~~1–7.5~~1–7.5 nm)[31,32] and a particle size distribution system (PSD; 3 ~~nm - 10 μm)~~nm–10 μm).[33]~~.~~ The DEG-SMPS was sampled through the northern window of the observation room. The aerosols entering the DEG-SMPS were sampled using a core sampling method with ~~~~100%~~~100% sampling ~~efficiency~~efficiency.[34]~~.~~ The DEG-SMPS was equipped with a soft X-ray neutralizer (TSI Inc., model 3088) for aerosol charging and a miniature cylindrical differential mobility analyzer (mini-cyDMA)[32] for sub-10 nm aerosol classification. Downstream of the mini-cyDMA, the DEG-UCPC was modified from a commercialized UCPC (TSI Inc., model 3776). The temperatures of the saturator and the condenser of the DEG-UCPC were 71 ~~°C~~ and 20 ~~°C,~~°C, respectively. The flow rates through the DEG-UCPC capillary and the saturator were 0.25 and 0.75 ~~L·min~~L·min$^{-1}$, respectively. A commercialized CPC was used to count the particles in the downstream of DEG-UCPC. The DEG-SMPS was calibrated four times a year using a homemade calibration ~~system~~system.[31]~~.~~ The PSD inlet was deployed downstream of a $PM_{10}$ impactor on the roof. The relative humidity was conditioned to be below 40% using a Nafion dryer (Perma Pure, ~~MD-700–24F-3)~~MD-700–24F-3) on the sampling line. The PSD consists of a TSI aerodynamic particle sizer (TSI Inc., model 3321) and two parallel SMPSs equipped with a TSI nanoDMA (TSI Inc., model 3085) and a TSI longDMA (TSI Inc., model 3081), respectively. The time resolution for particle size distribution measurement was 5 min.

The $H_2SO_4$ concentration was measured by a chemical ionization-atmospheric ~~interface-time-of-flight~~ interface-time-of-flight mass ~~spectrometers~~spectrometer (CI-APi-ToF, or CIMS; Aerodyne Research Inc.) equipped with ~~a~~ nitrate chemical ~~ionization~~ionization.[35–37]~~.~~ Before ~~Apr.~~April 14, 2018, the $H_2SO_4$ concentration was measured by a long time-of-flight mass spectrometer (CI-APi-LToF) and after that it was measured by a high-resolution time-of-flight mass spectrometer (CI-APi-HToF). Ambient air was taken into the CIMS through the north window. The sampling line was straight stainless-steel tubing with an outer diameter of 3/4 ~~inch.~~in. Before and after ~~Apr.~~April 14, the length of the sampling line was 1.6 ~~m~~ and 1.4 m, respectively, and the sampling flow rate was 8.8 ~~L·min$^{-1}$~~ and 8.5 ~~L·min~~L·min$^{-1}$, respectively. The sampling configurations during these two periods were similar ~~with~~to those previously described ~~in~~by Lu et al.[29]~~.~~ The $H_2SO_4$ concentration was calibrated using a homemade calibration ~~system~~system.[38]~~.~~ The calibration system produces $H_2SO_4$ from the oxidation of $SO_2$ by OH radicals. The transmission efficiency of the spectrometer was measured by adding different perfluorinated acids in amounts sufficient to deplete $NO_3^-$[39]~~.~~ The time resolution for the $H_2SO_4$ concentration was 5 min.

The meteorological data, including the temperature, ambient pressure, relative humidity, wind ~~speed~~speed, and wind direction, were measured by a local weather station (Vaisala, AWS310). Amine concentration was measured using a modified ToF-CIMS (Aerodyne Research, ~~Inc)~~Inc.) from ~~Oct.~~October 24, 2018 to ~~Mar.~~March 13, ~~2019~~2019.[18,40]~~. Duirng~~ During this period, the median concentration of the most abundant amine species, dimethylamine (DMA), was 2.7 ppt. The time resolution of the meteorological data and the amine concentration was 5 min.

The long-term field measurement started from ~~Jan.~~January 2018. In this study, we used the aerosol size distribution data on a total of 234 days in 2018 ~~(Jan. 16 – Apr.~~ (January 16–April 10, ~~Apr. 29 – May~~ April 29–May 17, May ~~22 – Dec.~~ 22–December 26) and a total of 48 days in 2019 summer (June ~~1 – Aug.~~ 1–August 31), covering winter ~~(Dec. – Feb.),~~ (December–February), spring ~~(Mar. – May),~~ (March–May), summer ~~(Jun. – Aug.)~~ (June–August), and autumn ~~(Sep. – Nov.).~~ (September–November). The $H_2SO_4$ concentration data were available on 131 days in 2018 ~~(Jan. 23 – Apr.~~ (January 23–April 10, ~~Oct. 20 – Dec.~~ October 20–December 26) and 67 days in 2019 summer ~~(Jun. 1 – Aug.~~ (June 1–August 13). Note that the data from the summer of 2019 were used to complement the analysis of NPF seasonal characteristics in urban Beijing. ~~Data~~ The data from the summer of 2018 were only used to evaluate NPF frequencies.

## 2.2~~.~~. Data ~~analysis~~Analysis

During these measurement periods, we classified all of the days into NPF days, undefined days, and non-NPF days. The classification criteria and examples are described in the ~~Supplementary Information (SI).~~Supplementary Information (SI).

The particle formation rate quantifies the growth flux through a certain particle diameter, which characterizes the intensity of NPF. In this study, the particle formation rate was calculated using a balance formula by Cai and ~~Jiang~~Jiang,[19] ~~,~~ which improves the estimation of coagulation scavenging in the presence of high aerosol loadings:

$$J_k = \frac{\mathrm{d}N_{[d_k,d_u)}}{\mathrm{d}t} + \sum_{d_g=d_k}^{d_{u-1}} \sum_{d_i=d_{\min}}^{+\infty} \beta_{(i,g)} N_{[d_i,d_{i+1})} N_{[d_g,d_{g+1})} - \frac{1}{2} \sum_{d_g=d_{\min}}^{d_{u-1}} \sum_{d_i^3=\max(d_{\min}^3,\, d_k^3-d_{\min}^3)}^{d_{i+1}^3+d_{g+1}^3 \le d_u^3} \beta_{(i,g)} N_{[d_i,d_{i+1})} N_{[d_g,d_{g+1})} + \left.\frac{\mathrm{d}N}{\mathrm{d}d_i}\right|_{d_i=d_u} \cdot \mathrm{GR}_u \quad (1)$$

~~Here~~Here, $J_k$ is the particle formation rate at size $d_k$, $cm^3$ ~~·s~~$s^{-1}$, with $d_k$ chosen to be 1.5 nm in this study, m; $d_u$ is the upper size limit of the targeted aerosol population, m; $d_{min}$ is the smallest particle size detected by particle size spectrometers, m; $N_{[d_k,d_u)}$ is the number concentration of particles from size $d_k$ to $d_u$, $cm^3$; $d_i$ represents the lower limit of the $i^{th}$ size bin, m; ~~β~~$\beta_{(i,g)}$ is the coagulation coefficient for the collision of two particles with the size of $d_i$ and $d_g$, $cm^3$ ~~·s~~$s^{-1}$; and $GR_u$ refers to the particle growth rate at size $d_u$, ~~nm·h~~$nm \cdot h^{-1}$.

The particle growth rate, GR, was obtained using the log-normal distribution function ~~method~~method, which tracks the temporal variation of the representative ~~diameter~~diameter.[41] ~~.~~ The growth rates in various particle size ranges, $GR_{1-3}$, $GR_{3-7}$~~3–7~~, $GR_{7-15}$~~7–15~~, and $GR_{15-25}$~~15–25~~, were calculated separately, where the subscripts indicate the size range (see the example given in Figure S2 in the ~~SI).~~ Supporting Information (SI)). Note that since the contribution of coagulation scavenging was not excluded, the obtained particle growth rates are apparent growth rates rather than growth rates resulting solely from the condensation onto individual ~~particles~~particles.[42] ~~.~~

The coagulation scavenging of particles was characterized using the condensation sink ~~(CS)~~(CS), which was calculated using ~~Equation~~eqs S1 and ~~Equation~~ S2 in the ~~SI~~SI.[41] ~~.~~ The influences of temperature and relative humidity on the diffusivity of $H_2SO_4$ were ~~corrected~~corrected.[43,44] ~~.~~

*I* is a ~~recently-proposed~~ recently proposed parameter that predicts the occurrence of atmospheric NPF dominated by $H_2SO_4$-amine nucleation in the presence of a high aerosol ~~loading~~loading.[24] ~~.~~ It is defined as

$$I = \frac{\beta^3 [\mathrm{A}_{1,\,\mathrm{tot}}]^4}{\mathrm{CS}^2} \eta^4 \quad (2)$$

where ~~β~~$\beta$ is the collision coefficient between two $(H_2SO_4)_1(amine)_1$ clusters, $cm^3$ ~~·s~~$s^{-1}$; $A_{1,tot}$ refers to the total concentration of measured $H_2SO_4$ monomer, $cm^3$; and CS is the condensation sink (note that the enhancement factor of coagulation between clusters due to van der Waals forces was taken into account, and this factor was estimated to be 2.3 and 1.3 for ~~β~~$\beta$ and CS, respectively), $s^{-1}$; ~~η~~$\eta$ is the ratio of the $(H_2SO_4)_1(amine)_1$ cluster concentration to the total $H_2SO_4$ monomer concentration given by

$$\eta = \frac{[\mathrm{A_1B_1}]}{[\mathrm{A_1}] + [\mathrm{A_1B_1}]} \approx \frac{\beta[\mathrm{B}]}{\gamma(T) + \mathrm{CS} + \beta[\mathrm{B}]} \quad (3)$$

here, $[A_1B_1]$ represents $(H_2SO_4)_1(amine)_1$ concentration, $cm^3$; $[A_1]$ is the concentration of $H_2SO_4$ molecules, $cm^3$; [B] indicates the amine concentration, $cm^3$; *T* is the temperature, K; ~~γ~~ and γ represents the evaporation rate of $(H_2SO_4)_1(amine)_1$ as a function of *T*, $s^{-1}$. Since $[A_1]$ and $[A_1B_1]$ cannot be directly measured using the current instruments, ~~η~~$\eta$ was calculated using the rightmost formula in eq 3. Since the

amine concentration was missing in winter and spring of 2018, a constant amine concentration, 2.7 ppt, which is the median of the measured amine concentration, was used when estimating ~~η~~η (see details in the SI). As a result, the analysis based on the indicator *I* mainly reflects the influence of the $H_2SO_4$ concentration, CS, and temperature. More details on ~~eqs~~eqs 2 ~~2~~ and ~~3~~3 are explained in the SI and by Cai et al.[24]~~.~~

## 3~~.~~. Results and ~~discussion~~Discussion

### 3.1~~.~~. Overall ~~characteristics~~Characteristics of NPF in ~~urban~~Urban Beijing

During our measurement periods, NPF event days and undefined days covered ~~37%~~37 and 6% of days, respectively. The daily maximum formation rate of 1.5 nm particles, $J_{1.5}$, during NPF periods ranged from 6 to 2200 cm~~$^{-3}$~~$^{-3}$~~·s~~·s$^{-1}$ with a median value of 79 cm~~$^{-3}$~~$^{-3}$~~·s~~·s$^{-1}$ (Figure 1). The values of GR~~1-3~~1–3, GR~~3-7~~3–7, GR~~7-15~~7–15, and GR~~15-25~~15–25 were in the ranges ~~0.2-2.4, 0.6-5.2, 1.1-8.0,~~0.2–2.4, 0.6–5.2, 1.1–8.0, and ~~0.4-8.8 nm h~~0.4–8.8 nm·h$^{-1}$, respectively, with medians of 0.9, 1.7, 2.8, and 2.9 ~~nm h~~nm·h$^{-1}$, respectively.

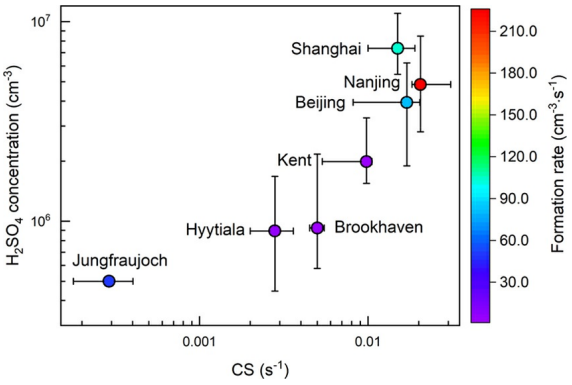


1~~.~~. ~~The~~ $H_2SO_4$ concentration and condensation sink in various atmospheric environments, including Beijing, ~~Nanjing~~Nanjing,[14]~~, Shanghai~~ Shanghai,[15]~~, Hyytiälä~~ Hyytiälä,[45]~~, Kent~~ Kent,[62]~~, Brookhaven~~ Brookhaven,[62] and ~~Jungraujoch~~Jungraujoch.[63,64]~~.~~ Data points in this figure are the median values and colored by the median formation rate of sub-2 nm particles. The error bars indicate the 25th and 75th percentiles, respectively. The $H_2SO_4$ concentration and CS in Beijing, Nanjing, ~~Shanghai~~Shanghai, and ~~Hyytiälä~~Hyytiälä are from long-term measurements ~~(≥ 7~~ (≥7 months). The $H_2SO_4$ concentration in Kent, ~~Brookhaven~~Brookhaven, and Jungfraujoch is from short-term measurements (<3 months). CS in Jungfraujoch is from a long-term measurement. CS in Kent and Brookhaven is from short-term measurements.

In urban Beijing, we observed new particle formation events characterized with a high $J_{1.5}$, high CS, and high $H_2SO_4$ concentration (Figure 1). The maximum value of $J_{1.5}$ measured during this study exceeded 1000 cm~~$^{-3}$~~$^{-3}$~~·s~~·s$^{-1}$, coinciding with the high $H_2SO_4$ concentration ~~(~2.5 ×~~(~2.5 × $10^7$ cm~~$^{-3}$~~$^{-3}$) observed during that NPF event ~~(Feb.~~(February 4, 2018). The aerosol loading, characterized by CS, was high in urban Beijing ~~compared~~compared to ~~to~~ those observed in relatively clean environments (Figure 1). The median value of CS during the NPF periods in urban Beijing was ~~~0.019~~~0.019 s$^{-1}$, while it was ~~~0.0025~~~0.0025 s$^{-1}$ in the Finnish boreal forest of ~~Hyytiälä~~Hyytiälä.[45]~~.~~ The high CS in urban Beijing implies that the scavenging loss rates of gaseous precursors, ~~clusters~~clusters, and newly formed particles are high. The median daily maximum $H_2SO_4$ concentration ~~the~~ during NPF periods in urban Beijing was ~~~4 ×~~~4 × $10^6$ cm~~$^{-3}$~~$^{-3}$, a factor of ~~~4~~~4 higher than those in cleaner environments but close to those in other megacities (Figure 1).

Note that after properly correcting for the coagulation scavenging effect using eq 1 and with direct measurement of sub-3 nm particles, $J_{1.5}$ reported in this study is higher than that reported in a previous long-term study in urban ~~Beijing~~Beijing.[17]~~.~~ Even with the same dataset of measured sub-3 nm particles, the formula used in previous studies underestimates the formation rate of 1.5 nm particles (Figure S3 in the SI). This discrepancy is mainly attributed to the fact that underestimating or neglecting the coagulation scavenging effect of small particles will underestimate the formation rate in atmospheric environments with ~~a~~ high aerosol ~~loading~~loading.[11]~~.~~ The high values of $J_{1.5}$ observed in this long-term measurement are consistent with the values recently reported in urban Beijing during a short-term field ~~campaign~~campaign.[11]~~.~~

From a global perspective, the new particle formation rate in polluted environments appears to be higher than that in relatively clean areas. As shown in Figures 1 and 2, the formation rates of ~~~1.5~~~1.5 nm particles in Chinese megacities, such as Beijing, Shanghai, and Nanjing,

are much higher than those in other relatively clean sites, such as the Finnish boreal forest of ~~Hyytiälä.~~Hyytiälä. The inferred nucleation rates were reported to be very high as well in other polluted megacities, such as Mexico City and Delhi (although the formation rate of ~~~1.5~~~1.5 nm particles in these places ~~were~~was not directly ~~measured)~~measured).[12,46,47]~~.~~ In addition, relatively high formation rates of ~~~1.5~~~1.5 nm particles were observed in Po Valley (Figure 2). Although Po Valley is labeled as a rural site, it is strongly influenced by anthropogenic emissions from the industrial areas and is surrounded by ~~the mountains~~mountains.[48]~~.~~ Its relatively high CS ~~(~ 0.011~~ (~0.011 $s^{-1}$) reflects the polluted characteristics of Po Valley.

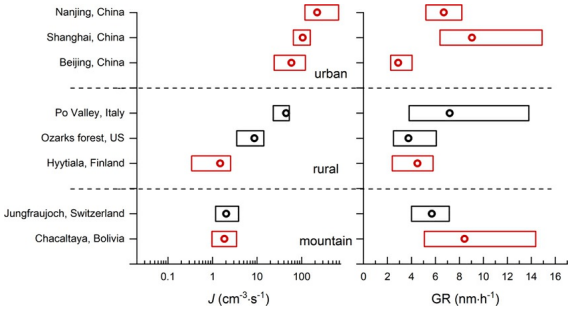


2~~.~~. Comparison of (a) the formation rate of sub-2 nm particles, *J*, and (b) the particle growth rate, $GR_{~~7-15~~7–15}$, in various environments, including Beijing (this study), ~~Nanjing~~Nanjing,[14]~~, Shanghai~~ Shanghai,[15]~~,~~ Po ~~Valley~~Valley,[48]~~, Ozarks~~ Ozarks,[65]~~, Hyytiälä~~ Hyytiälä,[66]~~,~~ ~~Jungfraujoch~~ Jungfraujoch,[63]~~,~~ and ~~Chacaltaya~~Chacaltaya.[51]~~.~~ Urban, ~~rural~~rural, and mountain environments are divided by dash lines. Data from long-term measurements ~~(≥ 7~~ (≥7 months) are shown by red color and the data from short-term field campaigns (<3 months) by black color. Circles represent median values. The left and right edges of bars are ~~25%~~25 and 75% percentiles, respectively, ~~expect~~except for Po Valley that ~~indicate 5%~~indicates 5 and 95% percentiles, respectively, and for ~~Hyytiälä~~Hyytiälä that indicate one standard deviation. $J_{1.5}$ is used for Beijing. $J_{1.4}$, $J_{1.7}$, $J_{1.6}$, and $J_1$ are used for Nanjing, Shanghai, Po Valley, and Ozark forest, respectively. $J_2$ is used for ~~Hyytiälä,~~Hyytiälä, Jungfraujoch, and Chacaltaya. $GR_{~~7-15~~7–15}$, $GR_{~~3-20~~3–20}$, and $GR_{~~5-25~~5–25}$ are used for Beijing, Nanjing, and Ozarks forest, respectively. $GR_{~~7-25~~7–25}$ is used for Shanghai and ~~Hyytiälä.~~Hyytiälä. $GR_{~~7-20~~7–20}$ is used for Po Valley, Jungfraujoch, and Chacaltaya.

Despite the high formation rate of ~~~1.5~~~1.5 nm particles, the observed growth rate in urban Beijing was relatively lower. The median value of $GR_{~~7-15~~7–15}$ was 2.8 ~~nm·h~~nm·h$^{~~-1~~1}$, which is lower than the median GR in many other environments (Figure 2). Such low GR, together with high CS, in urban ~~Beijing~~Beijing, may explain the observations that newly formed particles in urban Beijing sometimes cannot grow into very large ~~sizes~~sizes, although the formation rate is high (see ~~an~~the example in Figure S2). Note that uncertainties may be introduced when using different methods to estimate the observed GR. In addition, the observed GR is not equivalent to the condensational GR of an individual particle because the coagulation scavenging effect is not excluded when estimating the observed GR using the log-normal distribution function ~~method~~method.[42,49]~~.~~

### 3.2~~.~~. Seasonal ~~variations~~Variations of NPF ~~frequency~~Frequency and ~~formation rate~~Formation Rate in ~~urban~~Urban Beijing

The occurrence of NPF in urban Beijing had a strong seasonal variation (Figure 3). In winter, spring, summer, and autumn of 2018, the NPF frequencies were ~~51.4%, 25.4%, 16.7%~~51.4, 25.4, 16.7, and 30.2%, respectively. This is generally consistent with the previous observations in urban Beijing in the years of 2004[16] and ~~2008~~2008.[50]~~.~~ For these years, the NPF frequency was also the highest in ~~winter~~winter, whereas it was the lowest in summer. The lowest NPF frequency in summer was also observed in ~~Shanghai~~Shanghai.[15]~~.~~ In Chacaltaya, however, the NPF frequency was found to be the highest in ~~summer~~summer, whereas the lowest in ~~winter~~winter.[51]~~.~~ Similarly, in ~~Hyytiälä,~~Hyytiälä, the NPF event was often found to be the lowest in ~~winter~~winter.[52–54]~~.~~

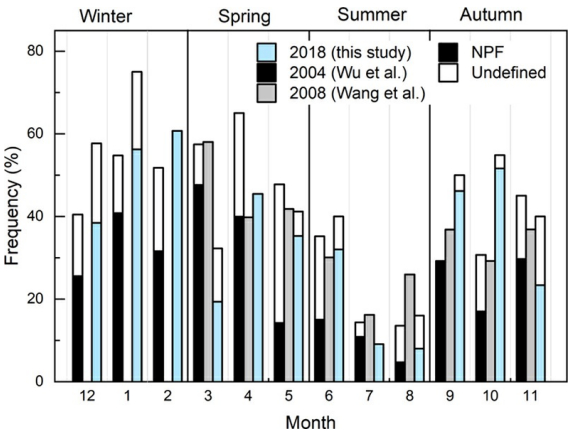


3~~.~~ . F~~The frequency~~requency of NPF days and undefined days during each month in urban Beijing for the years ~~of~~ 2018 (this study), ~~2008~~2008,[17]~~,~~ and ~~2004~~2004,[16]~~,~~ respectively. Black, ~~grey~~gray, and blue colors indicate the frequencies of NPF days for the years ~~of~~ 2004, ~~2008~~2008, and 2018, respectively. White color indicates the frequencies of undefined days. Note that the year ~~of~~ 2004 is from March 2004 to February 2005 as reported by Wu et al.[16]~~.~~

Similar to the observed variation of the NPF frequency in urban Beijing, the formation rate of 1.5 nm particles was much higher in winter than that in summer (Figure 4a). The seasonal cycle of formation rates is consistent with that observed previously in ~~Beijing~~Beijing,[16,17]~~,~~ although $J_3$ rather than $J_{1.5}$ was reported in those studies. The formation rate of 1.5 nm particles was also found to be the lowest in summer in ~~Shanghai~~Shanghai.[15]~~.~~ In ~~Hyytiälä,~~Hyytiälä, however, $J_{1.5}$ was estimated to be slightly higher in summer than in other seasons (although $J_{1.5}$ was estimated from a parametrization assuming heteromolecular nucleation between $H_2SO_4$ and oxidized ~~organics)~~organics).[53]~~.~~

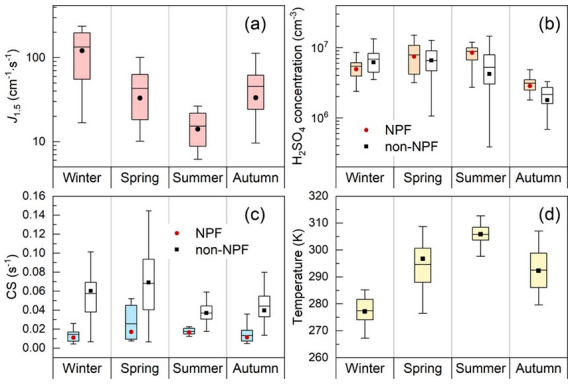


4~~.~~ . Seasonal variations of (a) the formation rate of 1.5 nm particles ($J_{1.5}$), (b) the $H_2SO_4$ concentration during NPF periods and non-NPF periods, (c) the condensation sink (CS) during NPF periods and non-NPF ~~periods~~periods, and (d) ambient temperature. ~~Colored~~ The colored and white box in (b) and (c) represent values during NPF periods and non-NPF periods, respectively. The bottom and top edges of the box indicate the 25th and 75th percentiles, respectively. The black line inside the box represents mean values. The circles and triangles indicate median values. CS values are the average during the NPF period on NPF days or ~~9:00-16:00~~9:00–16:00 on non-NPF days. Daily maximum values of $J_{1.5}$, $H_2SO_4$ concentration (both on NPF days and non-NPF days), and temperature are used in (a), (b), and (d), respectively.

The seasonal ~~variation~~variations of the $H_2SO_4$ concentration and CS in urban Beijing are very different from those of the NPF frequency and $J_{1.5}$. The $H_2SO_4$ concentration showed no obvious difference during NPF periods and non-NPF periods (Figure 4b). Instead, the daily maximum $H_2SO_4$ concentration was slightly higher in summer than that in winter. The seasonal variation of the $H_2SO_4$ concentration is different from those observed in Shanghai and ~~Hyytiälä~~Hyytiälä, where $H_2SO_4$ concentration was high in winter[15] and ~~spring~~spring,[53]~~,~~ respectively. In addition, CS showed no remarkable seasonal variation during the NPF periods in urban Beijing (Figure 4c). This is similar to observations made in ~~Shanghai~~Shanghai.[15]~~.~~ The median value of CS during the NPF periods in urban Beijing was ~~~0.019~~~0.019 s~~$^{-1}$~~$^{-1}$, approximately 3 times lower than the median CS value during non-NPF days ~~(~0.057~~(~0.057 s~~$^{-1}$~~$^{-1}$), further confirming that high pre-existing aerosols are able to suppress the occurrence of ~~NPF~~NPF.[11]~~.~~

Interestingly, the ambient temperature had an opposite seasonal cycle to that of the NPF frequency and $J_{1.5}$ in urban Beijing. Similar to other places, the ambient temperature in urban Beijing was the highest in summer and ~~the~~ lowest in winter (Figure 4d).

To explain the observed seasonal variation of $J_{1.5}$, we investigated the seasonal variation of the indicator *I*. The seasonal variation of the indicator *I* generally agreed with that of $J_{1.5}$ (see ~~Figure~~Figures 4a and ~~Figure~~ 5). This indicator is a function of the $H_2SO_4$ concentration, CS, and ambient temperature. Comparing *I* values estimated using both the measured temperatures and a constant temperature (275 K) during NPF periods, we found that the seasonal variation of the indicator *I* was mainly attributed to the seasonal variation of the ambient temperature (Figure 5).

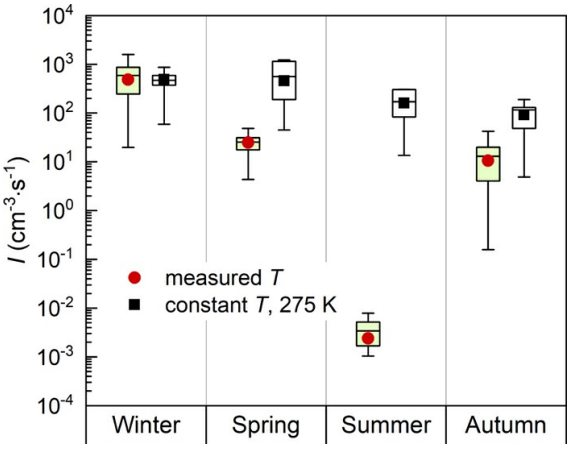


5~~.~~. Seasonal variations of the indicator, *I*, estimated at a constant ambient temperature of 275 K and the measured ambient temperature during NPF periods, respectively. The bottom and top edges of the box indicate the 25th and 75th percentiles, respectively. The black line inside the box represents the mean values. The dot and square markers indicate median values. Daily maximum values for *I* are used in this figure.

Based on the behavior of *I*, it seems likely that the seasonal variation of $J_{1.5}$ in urban Beijing was mainly driven by the seasonal variation of ambient temperature. $H_2SO_4$-amine nucleation governs new particle formation in urban ~~Beijing~~Beijing.[24,40] ~~The~~ The evaporation rate of $(H_2SO_4)_1(amine)_1$ clusters is a function of temperature (see ~~Equation~~eqs S3 and ~~Equation~~ S4 in the SI). In summer, the evaporation rate was the highest, whereas the ratio ~~(η)~~(η) of the $(H_2SO_4)_1(amine)_1$ cluster concentration to the total $H_2SO_4$ monomer concentration was the lowest (Figure S4 in the SI). The low values of ~~η~~η indicate that although the $H_2SO_4$ monomer concentration was high and CS was low in summer, it was still difficult for ~~a~~an NPF event to occur due to a high evaporation rate of $H_2SO_4$-amine clusters. Previous chamber studies reported that $H_2SO_4$-amine nucleation is rather insensitive to the temperature at high amine ~~concentrations~~concentrations.[55] ~~.~~ However, the above ~~evidences~~evidence and analysis in urban Beijing indicates that the temperature should be taken into ~~account,~~account because amine concentrations in urban Beijing are not high enough to make the formation rate of 1.5 nm particles insensitive to cluster ~~evaporation~~evaporation.[24] ~~.~~

Note that when estimating the values of *I* in Figure 5, a constant amine concentration of 2.7 ppt was ~~used~~used.[24,40] ~~.~~ When including the variations of amine concentration during the ~~five-month meausement,~~5-month measurement, ambient temperature still remained the main factor governing the seasonal variation of *I* values (see Figure S5 and related discussions in the SI). Nevertheless, long-term measurements of amines and other gaseous precursors are needed to further evaluate their contributions to the observed seasonal variations. Different from urban Beijing, the seasonal variation of the new particle formation rate in ~~Hyytiälä~~Hyytiälä was reported to be strongly related to the concentration variations of $H_2SO_4$ and ~~organics compounds~~organic compounds.[45] ~~. Evidences~~ Evidence from previous chamber studies and ambient measurements indicate that the nucleation process of $H_2SO_4$ molecules and oxidized organics are able to explain new particle formation in ~~Hyytiälä~~Hyytiälä.[56–58] ~~.~~ The differences in nucleation mechanisms and the governing factors possibly lead to the observed different seasonal variations of NPF frequency and formation rate in different places.

### 3.3~~.~~. Seasonal ~~variations~~Variations of ~~growth rate~~Growth Rate in ~~urban~~Urban Beijing

Despite the clear seasonal variations in the NPF frequency and $J_{1.5}$ in urban Beijing, the observed GRs in various size ranges were generally within the same range for all of the four seasons (Figure 6). Previous studies also reported no significant seasonal variations in the growth rate of nucleation mode ~~particles~~particles.[16,17] ~~.~~ Here, we further showed that the growth rates of sub-3 nm particles in four seasons are in ~~the~~a similar range, though with some variations. Similar to Beijing, the observed GR in Shanghai showed no clear seasonal variation, although the observed GR in Shanghai was higher than that in ~~Beijing~~Beijing.[15] ~~.~~ In ~~Hyytiälä,~~Hyytiälä, the observed GR was often

found to be the highest in summer, which is most likely related to the high abundance of biogenic volatile organic compounds at that time of the ~~year~~year.[45] ~~.~~ It is interesting to point out that the GR increases with an increasing particle size in urban Beijing, as reported ~~previously~~previously.[40] ~~.~~ A similar feature has been observed in a number of other sites as well, such as ~~Hyytiälä~~Hyytiälä,[41] ~~, Shanghai~~ Shanghai,[15] ~~,~~ Po ~~Valley~~Valley,[48] and ~~Chacaltaya~~Chacaltaya.[51] ~~.~~ This has been suggested to be caused by a reduced Kelvin effect with an increasing particle ~~size~~size.[59] ~~.~~

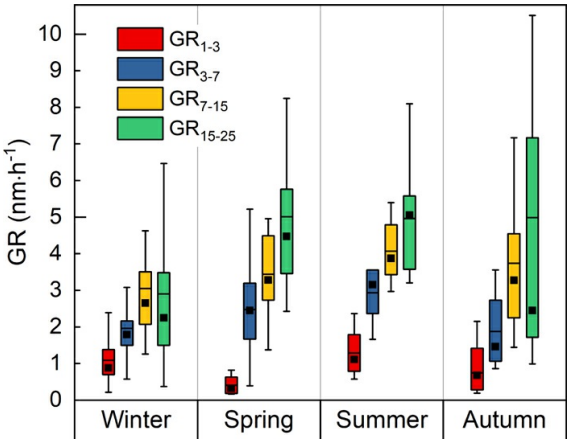


6~~.~~. Seasonal variations of the growth rates in various size ranges on NPF days. The bottom and top edges of the box indicate the 25th and 75th percentiles, respectively. The black line inside the box represents the mean values. The square markers indicate median values.

For all four seasons in urban Beijing, the condensation of $H_2SO_4$ and $(H_2SO_4)_{~~n~~n}$(amine)$_{~~n~~n}$ clusters ~~(n~~($n$ ~~≤~~≤ 4) ~~contribute~~contributes significantly to the observed GR of sub-3 nm particles with their minor seasonal variations (Figure 7a). Assuming kinetic condensation, the growth rate due to the condensation of $H_2SO_4$ and its clusters ($GR_{calculated}$) can be calculated as a function of particle size[60] (see the SI for details). As shown in Figure 7a, the ratios of the calculated $GR_{1-3}$ over the observed $GR_{~~1-3~~1–3}$ in all four seasons are close to 1, indicating that the condensation of $H_2SO_4$ and its clusters ~~contribute~~contributes significantly to the growth of particles in the sub-3 nm size range. These ratios are generally in the same range, though with some seasonal variations possibly related to the abundance of $H_2SO_4$ and its clusters in different seasons (Figure 4b) and the variations in the observed $GR_{~~1-3~~1–3}$ (Figure 6). The yearly data in urban Beijing also supports that the condensation of $H_2SO_4$ and stabilized $H_2SO_4$-base clusters ~~contribute~~contributes significantly to the measured GR for sub-3 nm particles (Figure S6a in the SI). This was observed in Shanghai[15] and in some controlled chamber conditions[28] as well. Note that there are uncertainties in both the calculated GR and the observed GR, especially in the sub-3 nm size range. For instance, the observed GR in the sub-3 nm size range is influenced by the estimation ~~method, and thus~~method and, thus, has an impact on the ratios of the calculated $GR_{~~1-3~~1–3}$ over the observed $GR_{~~1-3~~1–3}$. As shown in Figure S6b, a recently corrected appearance time method[21] gave higher values of the observed $GR_{~~1-3~~1–3}$ than the log-normal distribution function ~~method, and thus~~method and, thus, lower ratios. Nevertheless, results from both methods support that the condensation of $H_2SO_4$ and its clusters ~~contribute~~contributes significantly to the growth of particles in the sub-3 nm size range.

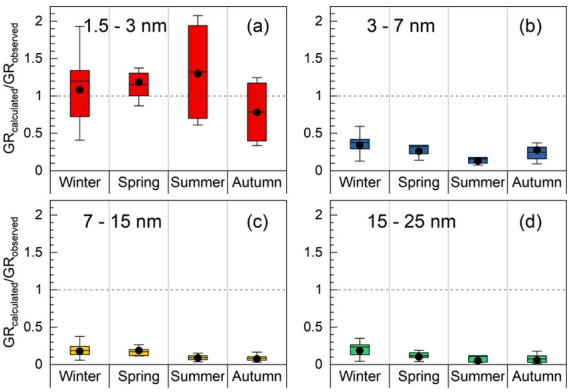


7~~.~~. R~~The ratio~~atio of the calculated growth rate ($GR_{calculated}$) over the observed growth rate ($GR_{observed}$) in four seasons for various size ranges: (a) ~~1.5 - 3~~1.5–3 nm, (b) ~~3 - 7~~3–7 nm, (c) ~~7 - 15 nm~~7–15 nm, and (d) ~~15 - 25~~15–25 nm. $GR_{calculated}$ estimated using the condensation of $H_2SO_4$ and $(H_2SO_4)_{~~n~~n}$(amine)$_{~~n~~n}$ clusters ~~(n~~($n$ ~~≤~~≤ 4). The geometric mean value of $GR_{calculated}$ in each size rage was used to calculate the ratio of $GR_{calculated}/GR_{observed}$. The bottom and top edges of the box indicate the 25th and 75th percentiles, respectively.

The black line inside the box represents the mean values. The dot markers indicate median values.

For all of the four seasons in urban Beijing, however, the condensation of $H_2SO_4$ and its clusters is less important for the growth rate of particles larger than 3 nm (Figure 7~~b–d),~~b–d), indicating the contributions of other species. In all seasons, the ratios of the calculated GR over the observed GR decreased as the particle size increased and are less than 25% for particles greater than 7 nm. Similar to the observed GR, there is no strong seasonal variations in these ratios. Other species, such as extremely low and low volatile compounds, ammonium and nitric acid, possibly contribute to the growth of these larger ~~particles~~particles.[40]~~.~~ In ~~Hyytiälä,~~Hyytiälä, for instance, extremely low-volatility organic compounds were found to be sufficient to explain the observed GR in larger size ~~ranges~~ranges.[27]~~.~~ As indicated ~~by~~in Figures 6 and 7, their total contribution to the observed GR in urban Beijing has no significant seasonal ~~variaiton.~~variation. To further investigate these gas species and their contributions, revealing that the chemical compositions of nanoparticles as they grow will be very helpful. Instruments such as the thermal desorption chemical ionization mass spectrometer (TDCIMS)[61] will be needed to directly measure the compositions of nanoparticles in this size range. It is also crucial to further understand the formation and physicochemical properties of low-volatility gas precursors (in addition to $H_2SO_4$ and its clusters).

With the measurement of aerosol size distributions down to ~~~1~~~1 nm, sulfuric acid, amines, and their clusters, we addressed the seasonal characteristics of new particle formation and its governing factors in the urban environment of Beijing. In contrast to the negligible influence of temperature on the $H_2SO_4$-amine nucleation in chamber studies at high amine ~~concentrations~~concentrations,[55]~~,~~ a strong temperature effect was observed under atmospheric conditions in urban Beijing. ~~Low-atmospheric~~ Low-atmospheric temperature favors the stability of $H_2SO_4$-amine ~~clusters, and thus~~clusters and, thus, the formation of new particles. Accordingly, the formation of 1.5 nm particles in urban Beijing showed a clear seasonal variation with maxima in winter and minima in summer. This may have implications on new particle formation within the global range since both seasonal variations and vertical variations in atmospheric temperature occur throughout the troposphere. Considering this effect in global models may lead to better ~~estimate~~ estimation of the budget of atmospheric aerosols and their ~~impacts~~impacts.[5]~~.~~ In contrast, the growth rates of both ~~sub-3~~ sub-3 nm particles and larger particles showed little seasonal variation in urban Beijing. While the condensation of $H_2SO_4$ and $H_2SO_4$-amine clusters ~~contribute~~contributes significantly to the growth of ~~sub-3~~ sub-3 nm particles in urban Beijing, its contribution to the observed growth rates decreases ~~rapdily~~rapidly as the particle size increases. This emphasizes the need to search for other condensing species that account for the growth of larger particles. In addition, the strong coagulation effect and the rich mixture of various gas precursors in the urban environment may have profound influences on particle ~~growth~~growth, which need to be further addressed.

## Supporting information

The supporting information is available free of charge on the ACS Publication website.

It includes the classification of NPF, ~~non-NPF~~non-NPF, and undefined days (Figure S1); ~~An~~an example for evaluating the observed growth rate (Figure S2); ~~The~~ calculation of the condensation sink ~~(Eq.~~(eqs S1 and ~~Eq.~~ S2); ~~The~~ comparison of the formation rate of 1.5 nm particles estimated using two formulae (Figure S3); ~~Details~~details on the indicator *I*; ~~The~~ calculation of the evaporation rate ~~(Eq.~~(eqs S3 and ~~Eq.~~ S4); ~~The~~ evaporation rate and ~~*η*~~*η* as a function of temperature in four seasons (Figure S4); ~~More~~more information on the measurement of amines and the influence of seasonal variation of amine concentration (Figure S5); ~~The~~ calculation of the growth rate due to the condensation of $H_2SO_4$ and its clusters ~~(Eq. S5, Eq. S6, Eq. S7 and Eq. S8); The~~ (eqs S5–S8); influence of seasonal variations of amine concentration ~~(Fig.~~(Figure S5); ~~The~~ ratio of the calculated growth rate ($GR_{calculated}$) over the observed growth rate ($GR_{observed}$) in various size ~~range~~ranges estimated using two different methods during these measurement periods ~~(Fig.~~(Figure S6) (PDF)

## Acknowledgments

Financial support from the National Key ~~R&D~~R&D Program of ~~China(2017YFC0209503),~~ China (2017YFC0209503), the National Science Foundation of China (21876094 ~~& 91643201)~~and 91643201), and Samsung $PM_{2.5}$ SRP are acknowledged. This project has received funding from the ERC ~~advanced grant No.~~Advanced Grant no. 742206, the European ~~Union's~~Union's Horizon 2020 research, and from the

Academy of Finland (Center of Excellence project no. 27204 and project no. 316114). We thank Zhengning Xu and Yuliang Liu for their help in sulfuric acid data in Nanjing.

## References

1Kulmala- M.- ~~Vehkamäki~~Vehkamäki- H.- ~~Petäjä~~Petäjä- T.- Dal Maso- M.- Lauri- A.- Kerminen- V. M.- Birmili- W.- McMurry- P. H.- Formation and growth rates of ultrafine atmospheric particles: a review of observations—— ~~Journal of~~ J . Aerosol ~~Science~~Sci.- 2004- 35- 2- 143- 176- 10.1016/j.jaerosci.2003.10.003.

2Zhang- R.- Khalizov- A.- Wang- L.- Hu- M.- Xu- W.- Nucleation and growth of nanoparticles in the atmosphere- ~~Chem Rev~~Chem. Rev.- 2012- 112- 3- 1957- 2011- 10.1021/cr2001756.

3Makkonen- R.- Asmi- A.- Kerminen- V. M.- Boy- M.- Arneth- A.- Hari- P.- Kulmala- M.- Air pollution control and decreasing new particle formation lead to strong climate warming- A~~Atmospheric Chemistry and Physics~~tmos. Chem. Phys.- 2012- 12- 3- 1515- 1524- 10.5194/acp-12-1515-2012.

4Kerminen- V.-M.- Lihavainen- H.- Komppula- M.- Viisanen- Y.- Kulmala- M.- Direct observational evidence linking atmospheric aerosol formation and cloud droplet activation- ~~Geophysical Research Letters~~Geophys. Res. Lett.- 2005- 32- 14- - L14803- 10.1029/2005GL023130.

5Merikanto- J.- Spracklen- D. V.- Mann- G. W.- Pickering- S. J.- Carslaw- K. S.- Impact of nucleation on global CCN- A~~Atmospheric Chemistry and Physics~~tmos. Chem. Phys.- 2009- 9- 21- 8601- 8616- 10.5194/acp-9-8601-2009.

6Dunne-, E. M.-; Gordon-, H.-; ~~Kä1/4rten~~Kürten-, A.-; Almeida-, J.-; Duplissy-, J.-; Williamson-, C.-; Ortega-, I. K.-; Pringle-, K. J.-; Adamov-, A.-; Baltensperger-, U.- *et al.* Global atmospheric particle formation from CERN CLOUD measurements-. ~~Science~~Science- 2016-, 354-6316- 1119- 1124-. 10.1126/science.aaf2649.

7Kerminen- V.-M.- Chen- X.- Vakkari- V.- ~~Petäjä~~Petäjä- T.- Kulmala- M.- Bianchi- F.- Atmospheric new particle formation and growth: review of field observations- E~~Environmental Research Letters~~nviron. Res. Lett.- 2018- 13- 10- - 103003- 10.1088/1748-9326/aadf3c.

8Chu- B.- Kerminen- V.-M.- Bianchi- F.- Yan- C.- ~~Petäjä~~Petäjä- T.- Kulmala- M.- Atmospheric new particle formation in China- A~~Atmospheric Chemistry and Physics~~tmos. Chem. Phys.- 2019- 19- 1- 115- 138- 10.5194/acp-19-115-2019.

9McMurry— P. H.— Friedlander— S. K.— New particle formation in the presence of an aerosol— ~~Atmospheric~~Atmos. Environ. ~~Environment~~ 1979- 13- 12- 1635- 1651- 10.1016/0004-6981(79)90322-6.

10Kerminen- V.-M.- Pirjola- L.- Kulmala- M.- How significantly does coagulational scavenging limit atmospheric particle production?- J~~Journal of Geophysical Research: Atmospheres~~. Geophys. Res.: Atmos.- 2001- 106- D20- 24119- 24125- 10.1029/2001JD000322.

11Cai- R.- Yang- D.- Fu- Y.- Wang- X.- Li- X.- Ma- Y.- Hao- J.- Zheng- J.- Jiang- J.- Aerosol surface area concentration: a governing factor in new particle formation in Beijing- A~~Atmospheric Chemistry and Physics~~tmos. Chem. Phys.- 2017- 17- 20- 12327- 12340- 10.5194/acp-17-12327-2017.

12Iida- K.- Stolzenburg- M. R.- McMurry- P. H.- Smith- J. N.- Estimating nanoparticle growth rates from size-dependent charged fractions: Analysis of new particle formation events in Mexico City— J~~Journal of Geophysical Research: Atmospheres~~. Geophys. Res.: Atmos.- 2008- 113- D5- - D05207- 10.1029/2007JD009260.

13Xiao- S.- Wang- M. Y.- Yao- L.- Kulmala- M.- Zhou- B.- Yang- X.- Chen- J. M.- Wang- D. F.- Fu- Q. Y.- Worsnop- D. R.- Wang- L.- Strong atmospheric new particle formation in winter in urban Shanghai, China— A~~Atmospheric Chemistry and Physics~~tmos. Chem. Phys.- 2015- 15- 4- 1769- 1781- 10.5194/acp-15-1769-2015.

14Yu- H.- Zhou- L.- Dai- L.- Shen- W.- Dai- W.- Zheng- J.- Ma- Y.- Chen- M.- Nucleation and growth of sub-3 nm particles in the polluted urban atmosphere of a megacity in China- A~~Atmospheric Chemistry and Physics~~tmos. Chem. Phys.- 2016- 16- 4- 2641- 2657- 10.5194/acp-16-2641-2016.

15Yao L. Garmash O. Bianchi F. Zheng J. Yan C. Kontkanen J. Junninen H. Mazon S. B. Ehn M. Paasonen P. Sipila M. Wang M. Wang X. Xiao S. Chen H. Lu Y. Zhang B. Wang D. Fu Q. Geng F. Li L. Wang H. Qiao L. Yang X. Chen J. Kerminen V. M. Petaja T. Worsnop D. R. Kulmala M. Wang L. Atmospheric new particle formation from sulfuric acid and amines in a Chinese megacity ScienceScience 2018 361 6399 278 281 10.1126/science.aao4839.

16Wu Z. Hu M. Liu S. Wehner B. Bauer S. Ma ßlingMassling A. Wiedensohler A. PetäjäPetäjä T. Dal Maso M. Kulmala M. New particle formation in Beijing, China: Statistical analysis of a 1-year data set JournalJ. Geophys. Res. of Geophysical Research 2007 112 D9 D09209 10.1029/2006JD007406.

17Wang Z. B. Hu M. Sun J. Y. Wu Z. J. Yue D. L. Shen X. J. Zhang Y. M. Pei X. Y. Cheng Y. F. Wiedensohler A. Characteristics of regional new particle formation in urban and regional background environments in the North China Plain AAtmospheric Chemistry and Physicstmos. Chem. Phys. 2013 13 24 12495 12506 10.5194/acp-13-12495-2013.

18Zheng J. Hu M. Zhang R. Yue D. Wang Z. Guo S. Li X. Bohn B. Shao M. He L. Huang X. Wiedensohler A. Zhu T. Measurements of gaseous H2SO4 by AP-ID-CIMS during CAREBeijing 2008 Campaign AAtmospheric Chemistry and Physicstmos. Chem. Phys. 2011 11 15 7755 7765 10.5194/acp-11-7755-2011.

19Cai R. Jiang J. A new balance formula to estimate new particle formation rate: reevaluating the effect of coagulation scavenging AAtmospheric Chemistry and Physicstmos. Chem. Phys. 2017 17 20 12659 12675 10.5194/acp-17-12659-2017.

20KürtenKürten A. Li C. Bianchi F. Curtius J. Dias A. Donahue N. M. Duplissy J. Flagan R. C. Hakala J. Jokinen T. Kirkby J. Kulmala M. Laaksonen A. Lehtipalo K. Makhmutov V. Onnela A. Rissanen M. P. Simon M. SipiläSipilä M. Stozhkov Y. TröstlTröstl J. Ye P. McMurry P. H. New particle formation in the sulfuric acid–dimethylamine–wateracid–dimethylamine–water system: reevaluation of CLOUD chamber measurements and comparison to an aerosol nucleation and growth model AAtmospheric Chemistry and Physicstmos. Chem. Phys. 2018 18 2 845 863 10.5194/acp-18-845-2018.

21Cai, R.; Li, C.; He, X. C.; Deng, C.; Lu, Y.; Yin, R.; Yan, C.; Wang, L.; Jiang, J.; Kulmala, M.; Kangasluoma, J. Impacts of coagulation on the appearance time method for sub-3 nm particle growth rate evaluation and their corrections. Atmos.Atmos. Chem. Phys. Discuss. Chem. Phys. Discuss. 2020, 2020, 1 24. 10.5194/acp-2020-398.

22McMurry P. H. Fink M. Sakurai H. Stolzenburg M. R. Mauldin R. L. Smith J. Eisele F. Moore K. Sjostedt S. Tanner D. Huey L. G. Nowak J. B. Edgerton E. Voisin D. A criterion for new particle formation in the sulfur-rich Atlanta atmosphere J.J. Geophys. Res. Geophys. Res. 2005 110 D22 1 10 10.1029/2005JD005901.

23Kuang C. Riipinen I. Sihto S. L. Kulmala M. McCormick A. V. McMurry P. H. An improved criterion for new particle formation in diverse atmospheric environments AAtmospheric Chemistry and Physicstmos. Chem. Phys. 2010 10 17 8469 8480 10.5194/acp-10-8469-2010.

24Cai, R.; Yan, C.; Yang, D.; Yin, R.; Lu, Y.; Deng, C.; Fu, Y.; Ruan, J.; Li, X.; Kontkanen, J.; Zhang, Q.; Kangasluoma, J.; Ma, Y.; Hao, J.; Worsnop, D. R.; Bianchi, F.; Paasonen, P.; Kerminen, V. M.; Liu, Y.; Wang, L.; Zheng, J.; Kulmala, M.; Jiang, J., SulfuricSulfuric Acid-Amine Nucleation in the[AQ1] Urban Atmospheric Environment acid-amine nucleation in the urban atmospheric environment., 2020., under review.(under review).

25Smith J. N. Moore K. F. Eisele F. L. Voisin D. Ghimire A. K. Sakurai H. McMurry P. H. Chemical composition of atmospheric nanoparticles during nucleation events in Atlanta JournalJ. Geophys. Res. of Geophysical Research 2005 110 D22 D22S03 10.1029/2005JD005912.

26Boy, M.; Kulmala, M.; Ruuskanen, T. M.; Pihlatie, M.; Reissell, A.; Aalto, P. P.; Keronen, P.; Maso, M. D.; Hellen, H.; Hakola, H. *et al.* Sulphuric acid closure and contribution to nucleation mode particle growth. AAtmospheric Chemistry and Physicstmos. Chem. Phys. 2005, 5 4 863 878, 10.5194/acp-5-863-2005.

27Ehn M. Thornton J. A. Kleist E. Sipila M. Junninen H. Pullinen I. Springer M. Rubach F. Tillmann R. Lee B. Lopez-Hilfiker F. Andres S. Acir I.

H.– Rissanen– M.– Jokinen– T.– Schobesberger– S.– Kangasluoma– J.– Kontkanen– J.– Nieminen– T.– Kurten– T.– Nielsen– L. B.– Jorgensen– S.– Kjaergaard– H. G.– Canagaratna– M.– Maso– M. D.– Berndt– T.– Petaja– T.– Wahner– A.– Kerminen– V. M.– Kulmala– M.– Worsnop– D. R.– Wildt– J.– Mentel– T. F.– A large source of low-volatility secondary organic aerosol- Nature- 2014- 506- 7489- 476- 9479- 10.1038/nature13032.

28Lehtipalo-, K.-; Rondo-, L.-; Kontkanen-, J.-; Schobesberger-, S.-; Jokinen-, T.-; Sarnela-, N.-; Kurten-, A.-; Ehrhart-, S.-; Franchin-, A.-; Nieminen-, T.-; Riccobono-, F.-; Sipila-, M.-; Yli-Juuti-, T.-; Duplissy-, J.-; Adamov-, A.-; Ahlm-, L.-; Almeida-, J.-; Amorim-, A.-; Bianchi-, F.-; Breitenlechner-, M.-; Dommen-, J.-; Downard-, A. J.-; Dunne-, E. M.-; Flagan-, R. C.-; Guida-, R.-; Hakala-, J.-; Hansel-, A.-; Jud-, W.-; Kangasluoma-, J.-; Kerminen-, V. M.-; Keskinen-, H.-; Kim-, J.-; Kirkby-, J.-; Kupc-, A.-; Kupiainen-Maatta-, O.-; Laaksonen-, A.-; Lawler-, M. J.-; Leiminger-, M.-; Mathot-, S.-; Olenius-, T.-; Ortega-, I. K.-; Onnela-, A.-; Petaja-, T.-; Praplan-, A.-; Rissanen-, M. P.-; Ruuskanen-, T.-; Santos-, F. D.-; Schallhart-, S.-; Schnitzhofer-, R.-; Simon-, M.-; Smith-, J. N.-; Trostl-, J.-; Tsagkogeorgas-, G.-; Tome-, A.-; Vaattovaara-, P.-; Vehkamaki-, H.-; Vrtala-, A. E.-; Wagner-, P. E.-; Williamson-, C.-; Wimmer-, D.-; Winkler-, P. M.-; Virtanen-, A.-; Donahue-, N. M.-; Carslaw-, K. S.-; Baltensperger-, U.-; Riipinen-, I.-; Curtius-, J.-; Worsnop-, D. R.-; Kulmala-, M.- The effect of acid-base clustering and ions on the growth of atmospheric nano-particles-. Nat CommunNat. Commun.- 2016-, 7-, 11594-. 11594. 10.1038/ncomms11594.

29Lu-, Y.-; Yan-, C.-; Fu-, Y.-; Chen-, Y.-; Liu-, Y.-; Yang-, G.-; Wang-, Y.-; Bianchi-, F.-; Chu-, B.-; Zhou-, Y.- *et al.* A proxy for atmospheric daytime gaseous sulfuric acid concentration in urban Beijing—. AAtmospheric Chemistry and Physicstmos. Chem. Phys.— 2019—, 19-3- 1971- 1983-, 10.5194/acp-19-1971-2019.

30Zhou- Y.- Dada- L.- Liu- Y.- Fu- Y.- Kangasluoma- J.- Chan- T.- Yan- C.- Chu- B.- Daellenbach- K. R.- Bianchi- F.- Kokkonen- T. V.- Liu- Y.- Kujansuu- J.- Kerminen- V. M.- PetäjäPetäjä- T.- Wang- L.- Jiang- J.- Kulmala- M.- Variation of size-segregated particle number concentrations in wintertime Beijing- Atmos.Atmos. Chem. Phys. Chem. Phys.- 2020- 20- 2- 1201- 1216- 10.5194/acp-20-1201-2020.

31Jiang- J.- Chen- M.- Kuang- C.- Attoui- M.- McMurry- P. H.- Electrical Mobility Spectrometer Using a Diethylene Glycol Condensation Particle Counter for Measurement of Aerosol Size Distributions Down to 1 nm— AAerosol Science and Technologyerosol Sci. Technol.- 2011- 45- 4- 510- 521- 10.1080/02786826.2010.547538.

32Cai- R.- Chen- D.-R.- Hao- J.- Jiang- J.- A miniature cylindrical differential mobility analyzer for sub-3 nm particle sizing- Journal of J. Aerosol ScienceSci.- 2017- 106- 111- 119- 10.1016/j.jaerosci.2017.01.004.

33Liu- J.- Jiang- J.- Zhang- Q.- Deng- J.- Hao- J.- A spectrometer for measuring particle size distributions in the range of 3 nm to 10 μmμm- FFrontiers of Environmental Science & Engineeringront. Environ. Sci. Eng.- 2016- 10- 1- 63- 72- 10.1007/s11783-014-0754-x.

34Fu- Y.- Xue- M.- Cai- R.- Kangasluoma- J.- Jiang- J.- Theoretical and experimental analysis of the core sampling method: Reducing diffusional losses in aerosol sampling line—— AAerosol Science and Technologyerosol Sci. Technol.- 2019- 53- 7- 793- 801- 10.1080/02786826.2019.1608354.

35Eisele- F.- Tanner- D.- Measurement of the gas phase concentration of H2SO4 and methane sulfonic acid and estimates of H2SO4 production and loss in the atmosphere—— JJournal of Geophysical Research: Atmospheres. Geophys. Res.: Atmos.- 1993- 98- D5- 9001- 9010- 10.1029/93JD00031.

36Bertram- T. H.- Kimmel- J. R.- Crisp- T. A.- Ryder- O. S.- Yatavelli- R. L. N.- Thornton- J. A.- Cubison- M. J.- Gonin- M.- Worsnop- D. R.- A field-deployable, chemical ionization time-of-flight mass spectrometer— AAtmospheric Measurement Techniquestmos. Meas. Tech.- 2011- 4- 7- 1471- 1479- 10.5194/amt-4-1471-2011.

37Jokinen- T.- SipiläSipilä- M.- Junninen- H.- Ehn- M.- LönnLönn- G.- Hakala- J.- PetäjäPetäjä- T.- Mauldin- R. L.- Kulmala- M.- Worsnop- D. R.- Atmospheric sulphuric acid and neutral cluster measurements using CI-APi-TOF- AAtmospheric Chemistry and Physicstmos. Chem. Phys.- 2012- 12- 9- 4117- 4125- 10.5194/acp-12-4117-2012.

38KürtenKürten- A.- Rondo- L.- Ehrhart- S.- Curtius- J.- Calibration of a chemical ionization mass spectrometer for the measurement of gaseous sulfuric acid- The Journal of Physical Chemistry J. Phys. Chem. A- 2012- 116- 24- 6375- 6386- 10.1021/jp212123n.

39Heinritzi M. Simon M. Steiner G. Wagner A. C. KürtenKürten A. Hansel A. Curtius J. Characterization of the mass dependent transmission efficiency of a CIMS AtAtmospheric Measurement Techniques mos. Meas. Tech. Discuss.Discussions 2015 8 11 1449 1460 10.5194/amtd-8-11369-2015.

40Yan, C.; Dada, L.; Dallenbach, K.; Kontkanen, J.; Yin, R.; Lu, Y.; Yang, D.; Fu, Y.; Deng, C.; Baalbaki, R.; Schervish, M.; Cai, J.; Cai, R.; Bloss, M.; Chan, T.; Chen, T.; Chen, Q.; Hakala, S.; Chen, X.; Chen, Y.; Chu, B.; Du, W.; Ezhova, E.; Fan, X.; Feng, Z.; Foreback, B.; Garmash, O.; Guo, Y.; He, X.; Heikkinen, L.; Hussein, T.; Jarvi, L.; Jokinen, T.; Junninen, H.; Kangasluoma, J.; Kokkonen, T.; Kurppa, M.; Lehtinen, K.; Li, C.; Li, H.; Li, H.; Li, X.; Liu, Y.; Ma, Q.; Nie, W.; Paasonen, P.; Pileci, R.; Qiao, X.; Rantala, P.; Rusanen, A.; Sarnela, N.; Simonen, P.; Stolzenburg, D.; Tilgner, A.; Tuovinen, S.; Vakkari, V.; Wang, L.; Wang, S.; Wang, W.; Wang, Y.; Wang, Y.; Xue, M.; Yang, D.; Yang, G.; Yao, L.; Zhang, H.; Zhang, G.; Zhang, Y.; Zheng, F.; Zeng, X.; Zhou, Y.; Zhouhui, L.; Kujansuu, J.; Petaja, T.; Zhang, S.; Ma, Y.; Ge, M.; He, H.; Donahue, N. M.; Worsnop, D. R.; Kerminen, V. M.; Ding, A.; Zheng, J.; Wang, L.; Liu, Y.; Jiang, J.; Bianchi, F.; Kulmala, M.; TheThe Birth of[AQ2] Haze birth of haze., 2020, under review.(under review).

41Kulmala M. Petaja T. Nieminen T. Sipila M. Manninen H. E. Lehtipalo K. Dal Maso M. Aalto P. P. Junninen H. Paasonen P. Riipinen I. Lehtinen K. E. Laaksonen A. Kerminen V. M. Measurement of the nucleation of atmospheric aerosol particles Nat ProtocNat. Protoc. 2012 7 9 1651 671667 10.1038/nprot.2012.091.

42Stolzenburg, M. R.; McMurry, P. H.; Sakurai, H.; Smith, J. N.; Mauldin, R. L.; Eisele, F. L.; Clement, C. F. Growth rates of freshly nucleated atmospheric particles in Atlanta. JJournal of Geophysical Research. Geophys. Res. 2005, 110D22 S05. S05. 10.1029/2005JD005935.

43Fuller E. N. Schettler P. D. Giddings J. C. New method for prediction of binary gas-phase diffusion coefficients Industrial & Engineering Chemistrynd. Eng. Chem. 1966 58 5 18 27 10.1021/ie50677a007.

44Hanson D. Eisele F. Diffusion of H2SO4 in humidified nitrogen: Hydrated H2SO4. TheH2SO4 Journal of Physical Chemistry J. Phys. Chem. A 2000 104 8 1715 1719 10.1021/jp993622j.

45Nieminen T. Asmi A. Maso M. D. Aalto P. P. Keronen P. Petaja T. Kulmala M. Kerminen V. M. Trends in atmospheric new-particle formation: 16 years of observations in a boreal-forest environment Boreal Environment ResearchEnviron. Res. 2014 19 1 191 214

46Kulmala M. PetäjäPetäjä T. MönkkönenMönkkönen P. Koponen I. K. Dal Maso M. Aalto P. P. Lehtinen K. E. J. Kerminen V. M. On the growth of nucleation mode particles: source rates of condensable vapor in polluted and clean environments Atmos.Atmos. Chem. Phys. Chem. Phys. 2005 5 2 409 416 10.5194/acp-5-409-2005.

47MönkkönenMönkkönen P. Koponen I. K. Lehtinen K. E. J. HämeriHämeri K. Uma R. Kulmala M. Measurements in a highly polluted Asian mega city: observations of aerosol number size distribution, modal parameters and nucleation events Atmos.Atmos. Chem. Phys. Chem. Phys. 2005 5 1 57 66 10.5194/acp-5-57-2005.

48Kontkanen J. JärvinenJärvinen E. Manninen H. E. Lehtipalo K. Kangasluoma J. Decesari S. Gobbi G. P. Laaksonen A. PetäjäPetäjä T. Kulmala M. High concentrations of sub-3nm clusters and frequent new particle formation observed in the Po Valley, Italy, during the PEGASOS 2012 campaign AAtmospheric Chemistry and Physicstmos. Chem. Phys. 2016 16 4 1919 1935 10.5194/acp-16-1919-2016.

49LeppäLeppä J. Anttila T. Kerminen V. M. Kulmala M. Lehtinen K. E. J. Atmospheric new particle formation: real and apparent growth of neutral and charged particles AAtmospheric Chemistry and Physicstmos. Chem. Phys. 2011 11 10 4939 4955 10.5194/acp-11-4939-2011.

50Wang Z. B. Hu M. Yue D. L. Zheng J. Zhang R. Y. Wiedensohler A. Wu Z. J. Nieminen T. Boy M. Evaluation on the role of sulfuric acid in the mechanisms of new particle formation for Beijing case AAtmospheric Chemistry and Physicstmos. Chem. Phys. 2011 11 24 12663 12671 10.5194/acp-11-12663-2011.

51Rose C. Sellegri K. Velarde F. Moreno I. Ramonet M. Weinhold K. Krejci R. Ginot P. Andrade M. Wiedensohler A. Laj P. Fre

quent nucleation events at the high altitude station of Chacaltaya (5240 m a.s.l.), Bolivia— AAtmospheric Environmenttmos. Environ.- 2015- 102- 18- 29- 10.1016/j.atmosenv.2014.11.015.

52Dal Maso- M.- Kulmala- M.- Riipinen- I.- Wagner- R.- Hussein- T.- Aalto- P. P.- Lehtinen- K. E.- Formation and growth of fresh atmospheric aerosols: eight years of aerosol size distribution data from SMEAR II, Hyytiala, Finland— Boreal Environment ResearchEnviron. Res.- 2005- 10- 5- 323

53Dada——— L.——— Paasonen——— P.——— Nieminen——— T.——— Buenrostro Mazon— S.— Kontkanen— J.— PeräkyläPeräkylä— O.— Lehtipalo— K.— Hussein— T.— PetäjäPetäjä— T.— Kerminen— V.-M.— BäckBäck— J.— Kulmala— M.— Long-term analysis of clear-sky new particle formation events and nonevents in HyytiäläHyytiälä- AAtmospheric Chemistry and Physicstmos. Chem. Phys.- 2017- 17- 10- 6227- 6241- 10.5194/acp-17-6227-2017.

54Nieminen-, T.-; Kerminen-, V.-M.-; PetäjäPetäjä-, T.-; Aalto-, P. P.-; Arshinov-, M.-; Asmi-, E.-; Baltensperger-, U.-; Beddows-, D. C. S.-; Beukes-, J. P.-; Collins-, D.-; Ding-, A.-; Harrison-, R. M.-; Henzing-, B.-; Hooda-, R.-; Hu-, M.-; HõrrakHõrrak-, U.-; KivekäsKivekäs-, N.-; Komsaare-, K.-; Krejci-, R.-; Kristensson-, A.-; Laakso-, L.-; Laaksonen-, A.-; Leaitch-, W. R.-; Lihavainen-, H.-; Mihalopoulos-, N.-; NémethNémeth-, Z.-; Nie-, W.-; amp;O'Dowd-, aposC. Dowd C.-; Salma-, I.-; Sellegri-, K.-; Svenningsson-, B.-; Swietlicki-, E.-; Tunved-, P.-; Ulevicius-, V.-; Vakkari-, V.-; Vana-, M.-; Wiedensohler-, A.-; Wu-, Z.-; Virtanen-, A.-; Kulmala-, M.- *et al.* Global analysis of continental boundary layer new particle formation based on long-term measurements-. AAtmospheric Chemistry and Physicstmos. Chem. Phys.- 2018-, 18-19- 14737- 14756-, 10.5194/acp-18-14737-2018.

55Almeida— J.— Schobesberger— S.— Kurten— A.— Ortega— I. K.— Kupiainen-Maatta— O.— Praplan— A. P.— Adamov— A.— Amorim— A.— Bianchi— F.— Breitenlechner— M.— David— A.— Dommen— J.— Donahue— N. M.——— Downard——— A.——— Dunne——— E.——— Duplissy——— J.——— Ehrhart——— S.——— Flagan——— R. C.- Franchin- A.- Guida- R.- Hakala- J.- Hansel- A.- Heinritzi- M.- Henschel- H.- Jokinen- T.- Junninen- H.- Kajos- M.- Kangasluoma- J.- Keskinen——— H.——— Kupc——— A.——— Kurten——— T.——— Kvashin——— A. N.— Laaksonen— A.— Lehtipalo— K.— Leiminger— M.— Leppa— J.— Loukonen— V.— Makhmutov— V.— Mathot— S.— McGrath— M. J.- Nieminen- T.- Olenius- T.- Onnela- A.- Petaja- T.- Riccobono- F.- Riipinen- I.- Rissanen- M.- Rondo- L.- Ruuskanen- T.- Santos- F. D.——— Sarnela——— N.——— Schallhart——— S.——— Schnitzhofer——— R.——— Seinfeld——— J. H.- Simon- M.- Sipila- M.- Stozhkov- Y.- Stratmann- F.- Tome- A.- Trostl- J.- Tsagkogeorgas- G.- Vaattovaara- P.- Viisanen- Y.- Virtanen- A.- Vrtala— A.— Wagner— P. E.— Weingartner— E.— Wex— H.— Williamson— C.— Wimmer— D.— Ye— P.— Yli-Juuti— T.— Carslaw— K. S.- Kulmala- M.- Curtius- J.- Baltensperger- U.- Worsnop- D. R.- Vehkamaki- H.- Kirkby- J.- Molecular understanding of sulphuric acid-amine particle nucleation in the atmosphere- Nature- 2013- 502- 7471- 359- 6363363- 10.1038/nature12663.

56Schobesberger— S.— Junninen— H.— Bianchi— F.— Lonn— G.— Ehn— M.— Lehtipalo— K.— Dommen— J.— Ehrhart— S.— Ortega— I. K.— Franchin— A.— Nieminen— T.— Riccobono— F.— Hutterli— M.— Duplissy— J.— Almeida— J.— Amorim— A.— Breitenlechner— M.— Downard— A. J.——————— Dunne——————— E. M.——————— Flagan——————— R. C.— Kajos— M.— Keskinen— H.— Kirkby— J.— Kupc— A.— Kurten— A.— Kurten— T.— Laaksonen— A.— Mathot— S.— Onnela— A.— Praplan— A. P.——————— Rondo——————— L.——————— Santos——————— F. D.- Schallhart- S.- Schnitzhofer- R.- Sipila- M.- Tome- A.- Tsagkogeorgas- G.- Vehkamaki- H.- Wimmer- D.- Baltensperger- U.- Carslaw- K. S.- Curtius- J.- Hansel- A.- Petaja- T.- Kulmala- M.- Donahue- N. M.- Worsnop- D. R.- Molecular understanding of atmospheric particle formation from sulfuric acid and large oxidized organic molecules— Proc Natl Acad Sci U S AProc. Natl. Acad. Sci. U.S.A.- 2013- 110- 43- 17223- 817228- 10.1073/pnas.1306973110.

57Metzger- A.- Verheggen- B.- Dommen- J.- Duplissy- J.- Prevot- A. S.- Weingartner- E.- Riipinen- I.- Kulmala- M.- Spracklen- D. V.- Carslaw- K. S.- Baltensperger- U.- Evidence for the role of organics in aerosol particle formation under atmospheric conditions- Proc Natl Acad Sci U S AProc. Natl. Acad. Sci. U.S.A.- 2010- 107- 15- 6646- 516651- 10.1073/pnas.0911330107.

58Lehtipalo-, K.-; Yan-, C.-; Dada-, L.-; Bianchi-, F.-; Xiao-, M.-; Wagner-, R.-; Stolzenburg-, D.-; Ahonen-, L. R.-; Amorim-, A.-; Baccarini-, A. J. S.- a.- Multicomponent new particle formation from sulfuric acid, ammonia, and biogenic vapors. Multicomponent new particle formation from sulfuric acid, ammonia, and biogenic vaporsSci. Adv.- 2018-, 4-12- eaau5363. 10.1126/sciadv.aau5363.

59Kuang, C., Chen, M., Zhao, J., Smith, J., McMurry, P. H., Wang, J. Size and time-resolved growth rate measurements of 1 to 5 nm freshly formed atmospheric nuclei, Atmospheric Chemistry and Physics, Atmos. Chem. Phys., 2012, 12, 7, 3573, 3589, 10.5194/acp-12-3573-2012.

60Stolzenburg, D., Simon, M., Ranjithkumar, A., Kürten, Kürten, A., Lehtipalo, K., Gordon, H., Nieminen, T., Pichelstorfer, L., He, X. C., Brilke, S., Xiao, M., Amorim, A., Baalbaki, R., Baccarini, A., Beck, L., Bräkling, Bräkling, S., Caudillo Murillo, L., Chen, D., Chu, B., Dada, L., Dias, A., Dommen, J., Duplissy, J., El Haddad, I., Finkenzeller, H., Fischer, L., Gonzalez Carracedo, L., Heinritzi, M., Kim, C., Koenig, T. K., Kong, W., Lamkaddam, H., Lee, C. P., Leiminger, M., Li, Z., Makhmutov, V., Manninen, H. E., Marie, G., Marten, R., Müller, Müller, T., Nie, W., Partoll, E., Petäjä, Petäjä, T., Pfeifer, J., Philippov, M., Rissanen, M. P., Rörup, Rörup, B., Schobesberger, S., Schuchmann, S., Shen, J., Sipilä, Sipilä, M., Steiner, G., Stozhkov, Y., Tauber, C., Tham, Y. J., Tomé, Tomé, A., Vazquez-Pufleau, M., Wagner, A. C., Wang, M., Wang, Y., Weber, S. K., Wimmer, D., Wlasits, P. J., Wu, Y., Ye, Q., Zauner-Wieczorek, M., Baltensperger, U., Carslaw, K. S., Curtius, J., Donahue, N. M., Flagan, R. C., Hansel, A., Kulmala, M., Volkamer, R., Kirkby, J., Winkler, P. M. Enhanced growth rate of atmospheric particles from sulfuric acid, Atmos. Atmos. Chem. Phys. Discuss., Chem. Phys. Discuss., 2019, 2019, 1, 17. 10.5194/acp-2019-755.

61Smith, J. N., Moore, K. F., McMurry, P. H., Eisele, F. L. Atmospheric Measurements of Sub-20 nm Diameter Particle Chemical Composition by Thermal Desorption Chemical Ionization Mass Spectrometry, Aerosol Science and Technology, Aerosol Sci. Technol., 2004, 38, 2, 100, 110, 10.1080/02786820490249036.

62Yu, H., Hallar, A. G., You, Y., Sedlacek, A., Springston, S., Kanawade, V. P., Lee, Y. N., Wang, J., Kuang, C., Mcgraw, R. L., *et al.* Sub-3 nm Particles Observed at the Coastal and Continental Sites in the United States, Journal of Geophysical Research: Atmospheres, Geophys. Res.: Atmos., 2014, 119, 2, 860, 879, 10.1002/2013JD020841.

63Boulon, J., Sellegri, K., Venzac, H., Picard, D., Weingartner, E., Wehrle, G., Collaud Coen, M., Bütikofer, Bütikofer, R., Flückiger, Flückiger, E., Baltensperger, U., Laj, P. New particle formation and ultrafine charged aerosol climatology at a high altitude site in the Alps (Jungfraujoch, 3580 m a.s.l., Switzerland), Atmospheric Chemistry and Physics, Atmos. Chem. Phys., 2010, 10, 19, 9333, 9349, 10.5194/acp-10-9333-2010.

64Bianchi, F., Trostl, J., Junninen, H., Frege, C., Henne, S., Hoyle, C. R., Molteni, U., Herrmann, E., Adamov, A., Bukowiecki, N., Chen, X., Duplissy, J., Gysel, M., Hutterli, M., Kangasluoma, J., Kontkanen, J., Ku rten, A., Manninen, H. E., Munch, S., Perakyla, O., Petaja, T., Rondo, L., Williamson, C., Weingartner, E., Curtius, J., Worsnop, D. R., Kulmala, M., Dommen, J., Baltensperger, U. New particle formation in the free troposphere: A question of chemistry and timing, Science, Science, 2016, 352, 6289, 1109, 12, 1112, 10.1126/science.aad5456.

65Yu, H., Ortega, J., Smith, J. N., Guenther, A. B., Kanawade, V. P., You, Y., Liu, Y., Hosman, K., Karl, T., Seco, R., Geron, C., Pallardy, S. G., Gu, L., Mikkilä, Mikkilä, J., Lee, S.-H. New Particle Formation and Growth in an Isoprene-Dominated Ozark Forest: From Sub-5 nm to CCN-Active Sizes, Aerosol Science and Technology, Aerosol Sci. Technol., 2014, 48, 12, 1285, 1298, 10.1080/02786826.2014.984801.

66Vana, M., Komsaare, K., Hõrrak, Hõrrak, U., Mirme, S., Nieminen, T., Kontkanen, J., Manninen, H. E., Petäjä, Petäjä, T., Noe, S. M., Kulmala, M. Characteristics of new-particle formation at three SMEAR stations, Boreal Environment Research, Environ. Res., 2016, 21, 3, 345, 362

# Supplementary Information

# Seasonal characteristics of new particle formation and growth in urban Beijing

*Chenjuan Deng[1], Yueyun Fu[1], Lubna Dada[2], Chao Yan[2,3], Runlong Cai[1], Dongsen Yang[4], Ying Zhou[3], Rujing Yin[1], Yiqun Lu[5], Xiaoxiao Li[1], Xiaohui Qiao[1], Xiaolong Fan[3], Wei Nie[6], Jenni Kontkanen[2], Juha Kangasluoma[2,3], Biwu Chu[2,3], Aijun Ding[6], Veli-Matti Kerminen[2], Pauli Paasonen[2], Douglas R. Worsnop[2,7], Federico Bianchi[2], Yongchun Liu[3], Jun Zheng[4], Lin Wang[5], Markku Kulmala[2,3,*], Jingkun Jiang[1,*]*

[1]State Key Joint Laboratory of Environment Simulation and Pollution Control, School of Environment, Tsinghua University, 100084 Beijing

[2]Institute for Atmospheric and Earth System Research/Physics, Faculty of Science, University of Helsinki, 00014 Helsinki, Finland

[3]Aerosol and Haze Laboratory, Beijing Advanced Innovation Center for Soft Matter Science and Engineering, Beijing University of Chemical Technology, 100029 Beijing, China

[4]Collaborative Innovation Center of Atmospheric Environment and Equipment Technology, Nanjing University of Information Science and Technology, 210044 Nanjing, China

[5]Shanghai Key Laboratory of Atmospheric Particle Pollution and Prevention (LAP3), Department of Environmental Science and Engineering, Fudan University, Shanghai 200433, China

[6]Joint International Research Laboratory of Atmospheric and Earth System Sciences, School of Atmospheric Sciences, Nanjing University, 210023 Nanjing, China

[7]Aerodyne Research Inc., Billerica, Massachusetts 01821, USA

**9 pages**

**6 figures**

## 1. Classification of NPF days, non-NPF days and undefined days

A typical NPF day is characterized as that there is a burst in the sub-3 nm particle number concentration ($N_{sub\text{-}3}$) and subsequent growth of these newly formed particles (usually lasts for several hours), e.g., the event shown in Fig. S1(a). If the burst of sub-3 nm particles is not followed by further particle growth, the day is classified as an undefined day (e.g., Fig. S1(b)). When neither the burst of sub-3 nm particles nor the subsequent growth of newly formed particles were observed, it was classified into a non-NPF day (e.g., Fig. S1(c)).

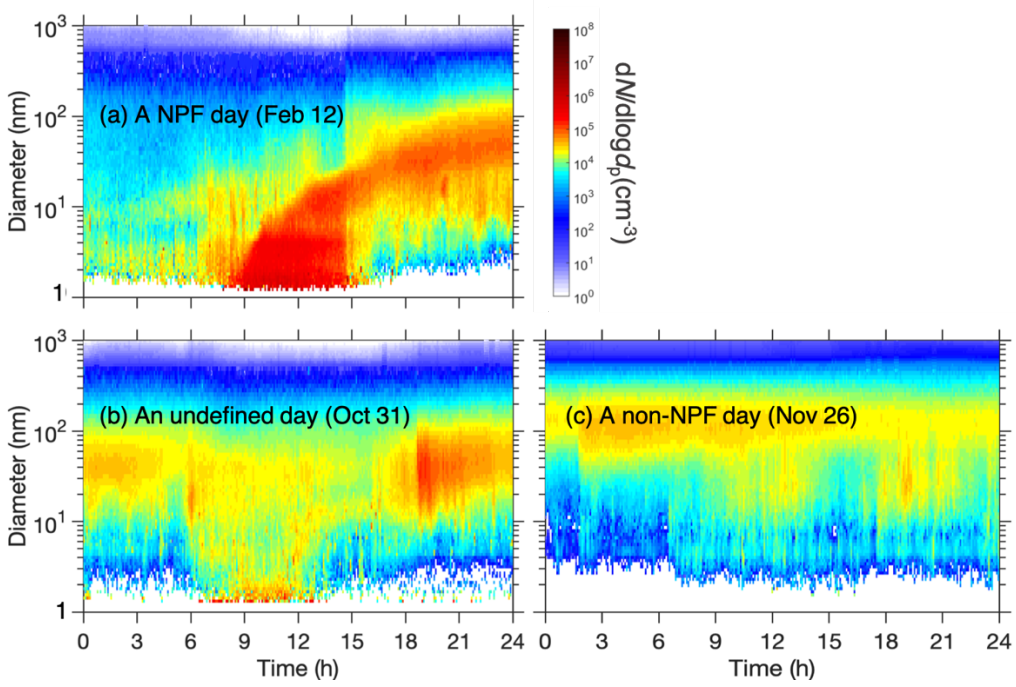


**Figure S1.** Typical particle size distributions of (a) a NPF day (Feb. 12, 2018), (b) an undefined day (Oct. 31, 2018), and (c) a non-NPF day (Nov. 26, 2018). The colored pixels represent aerosol number size distribution functions, d$N$/dlog$d_p$.

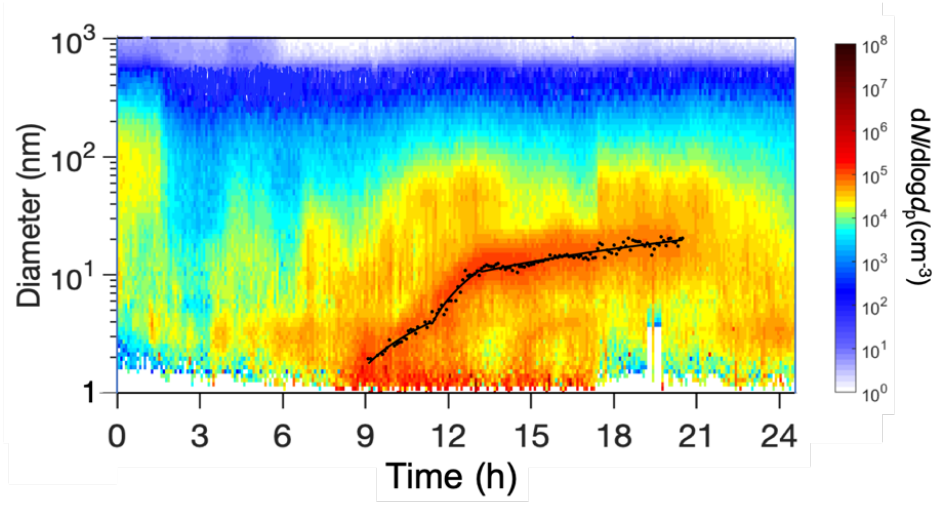


**Figure S2.** Lognormal fitting for estimating the observed growth rate on a NPF day (Feb. 14, 2018). Black dots are the representative diameter obtained through lognormal fitting to the measured aerosol size distributions during NPF periods. Black lines are obtained by linearly fitting the black dots. GR is calculated as the slope of the fitted black line, i.e., the gradient of the representative diameter as a function of time.

## 2. Calculation of the condensation sink

The condensation sink (CS) characterizes the condensing vapor sink caused by pre-existing aerosols and can be calculated using the method reported in Kulmala et al.[1],

$$CS = 2\pi D \sum_{d_p} \beta_{m,d_p} d_p N_{d_p} \quad \text{(S1)}$$

where $D$ is the diffusion coefficient of $H_2SO_4$, $m^2 \cdot s^{-1}$; $d_p$ is the particle geometric mean diameter for the size bin, m; $N_{d_p}$ is the concentration of particles in the size bin, $m^{-3}$; $\beta_m$ is the transition-regime correction factor[2],

$$\beta_m = \frac{1 + K_n}{1 + 1.677K_n + 1.333{K_n}^2} \quad \text{(S2)}$$

where $K_n$ is the Knudsen number, $K_n = 2\lambda/d_p$.

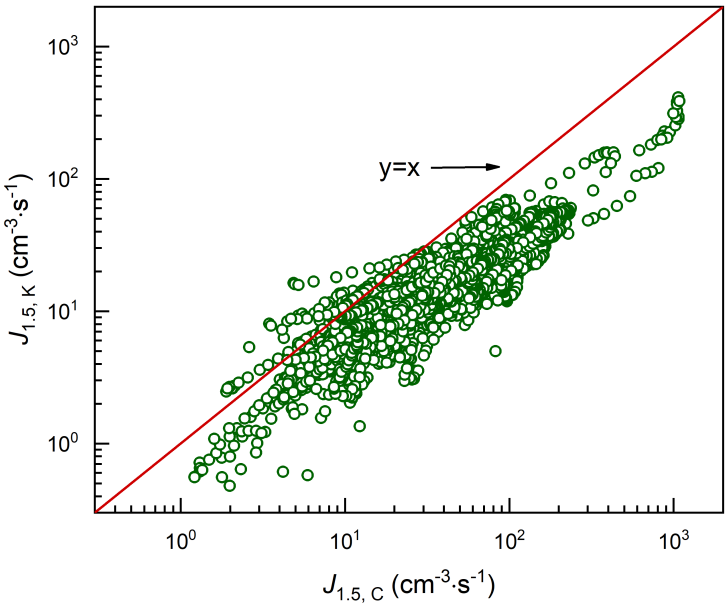


**Figure S3.** The formation rate of 1.5 nm particles estimated using two formulae, i.e., $J_{1.5,\,C}$ and $J_{1.5,\,K}$ were estimated using the equation (1) in Cai and Jiang[3] and the equation (10) in Kulmala et al.[1], respectively. Note that the formula in Kulmala et al.[1] was often used by previous studies to estimate the formation rate in urban Beijing[4, 5].

## 3. The indicator *I* for $H_2SO_4$-amine nucleation

Derived from the kinetic model[6], *I* is an indicator to predict the occurrence of NPF dominated by $H_2SO_4$-amine nucleation. It is a simplified form of the modeled formation rate of $H_2SO_4$ tetramers (see the SI in Cai et al.[6]). Reasonable approximations were made when deriving this indicator. Due to these approximations, *I* can be considered as an empirical indicator instead of the simulated formation rate. In urban Beijing, NPF days and non-NPF days can be well distinguished using this indicator[6].

When estimating $I$ using Eq. (2), the evaporation rate of $(H_2SO_4)_1(amine)_1$ cluster, γ, can be estimated from the collision rates and the Gibbs free energy of $(H_2SO_4)_1(amine)_1$ formation[6, 7],

$$\gamma(T) = \frac{\beta_{A_1B_1} p}{k_b T} \exp\left\{\frac{\Delta_f G_{m,A_1B_1}{}^{\theta}(T)}{RT}\right\} \quad \text{(S3)}$$

where $\gamma(T)$ is the evaporate rate, $s^{-1}$; $\beta_{A_1B_1}$ is the collision rate between the $H_2SO_4$ molecule and the amine molecule, $cm^{-3}\cdot s^{-1}$; $p$ is the atmospheric pressure, Pa; $k_b$ is the Boltzmann constant, $J\cdot K^{-1}$; $T$ is the atmospheric temperature, K; R is the ideal gas constant, $J\cdot mol^{-1}\cdot K^{-1}$; $\Delta_f G_{m,A_1B_1}{}^{\theta}(T)$ is the molar Gibbs free energy of $(H_2SO_4)_1(amine)_1$ formation at temperature $T$, $J\cdot mol^{-1}$. It can be calculated from the standard molar free energy of formation of $(H_2SO_4)_1(amine)_1$ at 298.15 K as shown in Eq. S4,

$$\frac{\Delta_f G_{m,A_1B_1}{}^{\theta}(T)}{T} = \frac{\Delta_f G_{m,A_1B_1}{}^{\theta}(T_0)}{T_0} - \int_{T_0}^{T} \frac{\Delta_f H_m{}^{\theta}}{T} d\bar{T} \quad \text{(S4)}$$

where $T_0$=298.15 K; $\Delta_f H_m{}^{\theta}$ is the standard molar enthalpy of formation of $(H_2SO_4)_1(amine)_1$, $J\cdot mol^{-1}$; $\Delta_f G_{m,A_1B_1}{}^{\theta}(T_0)$ is assumed to be -14.0 $kcal\cdot mol^{-1}$ in this study, which is fitted to the measured data in urban Beijing in a previous study[6]. Note that although this value is close to the latest quantum chemistry calculation results[8], there might be noticeable uncertainties in the calculated evaporation rates when T > 300 K because of lacking experimental data.

When estimating $\beta$ and CS needed in Eq. (3) to calculate $\eta$, the enhancement factors of coagulation due to van der Waals forces were taken into account. They were estimated using the method from Chan and Mozurkewich[9], which includes the effect of enhanced collision rates through van der Waals forces[10, 11]. The Hamaker constant was assumed to be 6.4×10-20 J[12]. The enhancement factors for $\beta$ and CS were estimated to be 2.3 and 1.3, respectively. The value of 2.3 has been shown to be consistent with the results obtained using atomistic simulation[13].

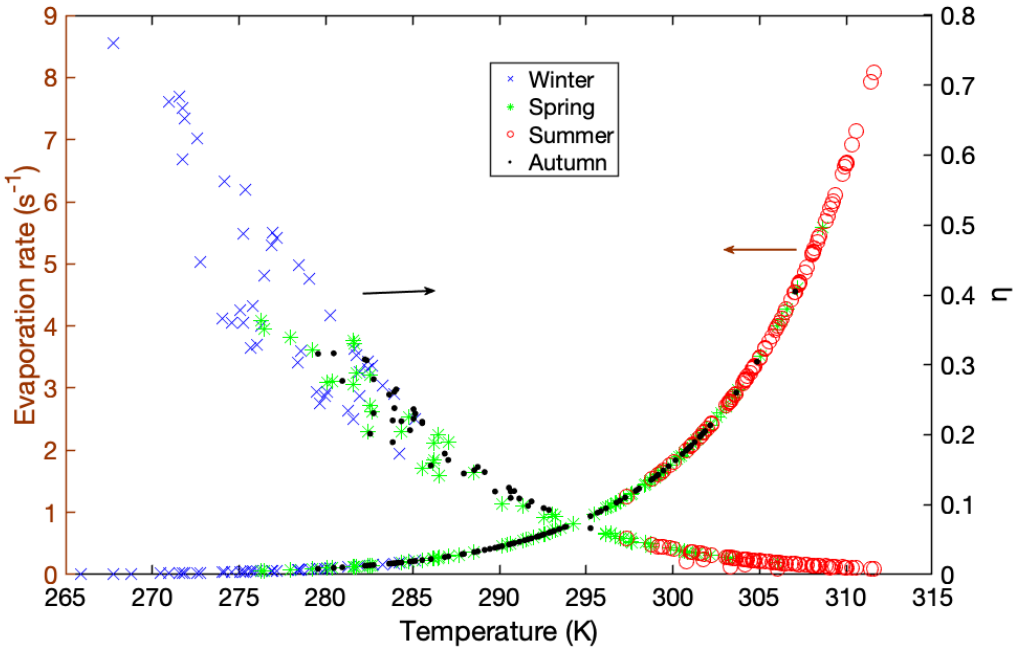


**Figure S4.** The evaporation rate (left) and the ratio of the $(H_2SO_4)_1(amine)_1$ cluster concentration to the total $H_2SO_4$ monomer concentration, $\eta$, as a function of atmospheric temperature in

various seasons. Blue cross, green asterisk, red circle, and black dot markers represent data in winter, spring, summer, and autumn, respectively.

## 4. The influence of seasonal variations of amine concentration

A broad range of amines were measured using a modified Aerodyne high resolution time-of-flight chemical ionization mass spectrometer (HR-ToF-CIMS)[14]. It also measures ammonia and amides. The ion chemistry is based on the proton-transfer reaction (PTR) between amines/ammonia and hydronium ions ($H_3O^+ \cdot (H_2O)_{n=0,1...}$). The construction, operation, and calibration of the instrument have been previously reported[14]. The concentrations of ammonia, three most abundant amines (methylamine (MA), dimethylamine (DMA), and trimethylamine (TMA)) and two amides were calibrated using a temperature-controlled U-shaped glass tube and the corresponding commercial permeation tubes. Note that the measured concentration of C2-amines was assumed to be the DMA concentration, which is most likely dominating in urban atmospheric environment over its isomer, ethylamine[15].

Atmospheric amine concentrations in urban Beijing have not been reported before, and observations of amine concentrations are also limited in other atmospheric environments around the world[16-20]. In our studies, the concentrations of amines were continuously measured for approximately 5 months. DMA was the most abundant one, with a median concentration of 2.7 ppt. Due to its abundancy and strong ability to stabilize $H_2SO_4$ clusters, DMA was shown to be the major stabilizing species in urban Beijing[6]. Hence, when estimating the indicator *I*, "amine" represents DMA and its concentration was set to be the median value of 2.7 ppt.

If we categorized five-month data into different seasons, the median DMA concentration in autumn (Oct. 24, 2018 – Nov. 30, 2018), winter (Dec. 1, 2018 – Feb. 28, 2019) and spring (Mar. 1, 2019 – Mar. 13, 2019) were ~4.1, 1.5, and 0.7 ppt, respectively. The range of 0.7-4.1 ppt was used to test the influence of amine concentration on the value of *I*. As shown in Fig. S5, the influence of amine concentration on *I* is less significant than ambient temperature.

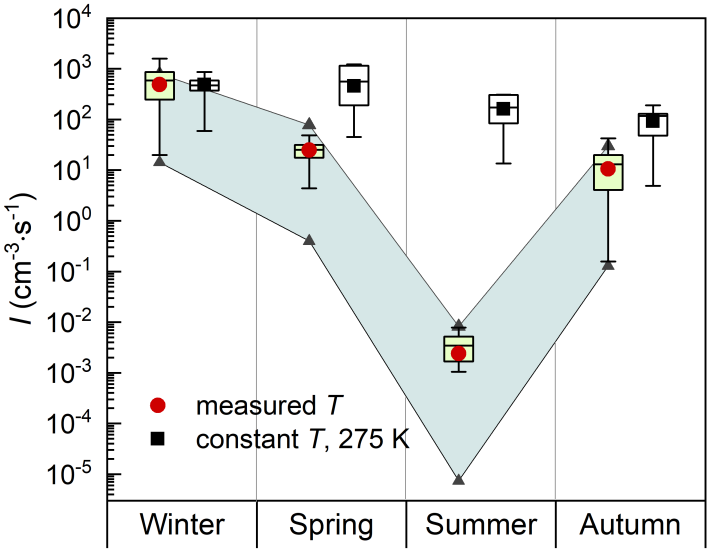


**Figure S5.** Seasonal variations of the indicator, *I*, estimated at a constant ambient temperature of 275 K and the measured ambient temperature during NPF periods, respectively. Daily maximum values for *I* were used in this figure. The bottom and top edges of the box indicate the 25th and 75th percentiles, respectively. The black line inside the box represents the mean values. The dot,

triangle and square markers indicate median values. The light blue shadow area represents the variation range of $I$ values estimated with the amine concentration in the range of 0.7-4.1 ppt.

## 5. Calculation of the calculated growth rate due to $H_2SO_4$ and clusters condensation

The growth rate due to the condensation of species ($H_2SO_4$ and $(H_2SO_4)_n(amine)_n$ clusters ($n \leq 4$)) can be calculated using the following equation,

$$GR = k_{coll} C_v \left[ \left( {d_p}^3 + {d_v}^3 \right)^{1/3} - d_p \right] \quad \text{(S5)}$$

where $d_p$ and $d_v$ represent the particle and vapor diameter, respectively, m; $k_{coll}$ represents the kinetic collision coefficient between particle and vapor, $m^3 \cdot s^{-1}$; $V_v$ is the volume of vapor molecule, $m^3$; $C_v$ is the concentration of condensing species, $m^{-3}$. The concentrations of $(H_2SO_4)_n(amine)_n$ clusters ($n \leq 4$) are derived using the simplified kinetic model in Cai et al.[6]. The accommodation coefficient is assumed to be unity. A collision enhancement of neutral vapors and particles due to attractive London-van-der-Waals forces is used when estimating $k_{coll}$[9, 11],

$$k_{coll}(d_v, d_p) = k_K \left( \sqrt{1 + \left( \frac{k_K}{k_D} \right)^2} \right) - \frac{k_K}{k_D} \quad \text{(S6)}$$

where $k_K$ and $k_D$ are the kinetic collision rates for the free molecule and continuum regime, respectively, and can be calculated as follows,

$$k_K = \frac{\pi}{8} \left( d_v + d_p \right)^2 \left( \frac{8kT}{\pi} \right)^{\frac{1}{2}} \left( \frac{1}{m_v} + \frac{1}{m_p} \right)^{\frac{1}{2}} E(\infty) \quad \text{(S7)}$$

$$k_D = 2\pi \left( d_v + d_p \right) \left( D_v + D_p \right) E(0) \quad \text{(S8)}$$

where $m_v$ and $m_p$ are the mass of the single condensing species and particle, respectively, kg; $D_v$ and $D_p$ are diffusion coefficient of condensing species and particles, respectively, $m^2 \cdot s^{-1}$. $E(\infty)$ and $E(0)$ are collision enhancement factors due to London-van-der-Waals forces and can be found in Chan and Mozurkewich[9].

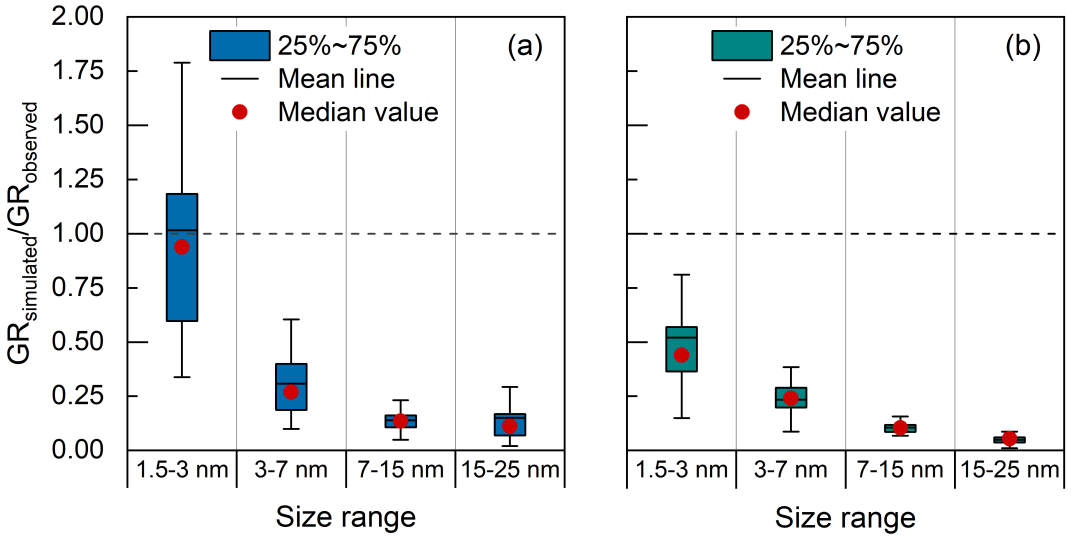


**Figure S6.** The ratio of the calculated growth rate ($GR_{calculated}$) over the observed growth rate ($GR_{observed}$) in various size range during these measurement periods. $GR_{observed}$ reported in (a) was estimated using the log-normal distribution function method. $GR_{observed}$ reported in (b) was estimated using the corrected appearance time method[21] in (b), respectively. Their differences indicate the influences in the observed GR caused by the estimation methods. $GR_{calculated}$ estimated using the condensation of $H_2SO_4$ and $(H_2SO_4)_n(amine)_n$ clusters ($n \leq 4$). The geometric mean value of $GR_{calculated}$ in each size rage was used to calculate the ratio of $GR_{calculated}/GR_{observed}$. The bottom and top edges of the box indicate the 25th and 75th percentiles, respectively. The black line inside the box represents the mean values. The dot and square markers indicate median values.

## Reference


1. Kulmala, M.; Petaja, T.; Nieminen, T.; Sipila, M.; Manninen, H. E.; Lehtipalo, K.; Dal Maso, M.; Aalto, P. P.; Junninen, H.; Paasonen, P.; Riipinen, I.; Lehtinen, K. E.; Laaksonen, A.; Kerminen, V. M., Measurement of the nucleation of atmospheric aerosol particles. *Nat Protoc* **2012,** *7*, (9), 1651-67.
2. Fuchs, N. A.; Sutugin, A. G., HIGH-DISPERSED AEROSOLS. In *Topics in Current Aerosol Research*, Hidy, G. M.; Brock, J. R., Eds. Pergamon: 1971; p 1.
3. Cai, R.; Jiang, J., A new balance formula to estimate new particle formation rate: reevaluating the effect of coagulation scavenging. *Atmospheric Chemistry and Physics* **2017,** *17*, (20), 12659-12675.
4. Wu, Z.; Hu, M.; Liu, S.; Wehner, B.; Bauer, S.; Ma ßling, A.; Wiedensohler, A.; Petäjä, T.; Dal Maso, M.; Kulmala, M., New particle formation in Beijing, China: Statistical analysis of a 1-year data set. *Journal of Geophysical Research* **2007,** *112*, (D9), D09209.
5. Wang, Z. B.; Hu, M.; Sun, J. Y.; Wu, Z. J.; Yue, D. L.; Shen, X. J.; Zhang, Y. M.; Pei, X. Y.; Cheng, Y. F.; Wiedensohler, A., Characteristics of regional new particle formation in urban and regional background environments in the North China Plain. *Atmospheric Chemistry and Physics* **2013,** *13*, (24), 12495-12506.
6. Cai, R.; Yan, C.; Yang, D.; Yin, R.; Lu, Y.; Deng, C.; Fu, Y.; Ruan, J.; Li, X.; Kontkanen, J.; Zhang, Q.; Kangasluoma, J.; Ma, Y.; Hao, J.; Worsnop, D. R.; Bianchi, F.; Paasonen, P.; Kerminen, V. M.; Liu, Y.; Wang, L.; Zheng, J.; Kulmala, M.; Jiang, J., Sulfuric acid-amine nucleation in the urban atmospheric environment. **2020. (under review)**.
7. McGrath, M. J.; Olenius, T.; Ortega, I. K.; Loukonen, V.; Paasonen, P.; Kurtén, T.; Kulmala, M.; Vehkamäki, H., Atmospheric Cluster Dynamics Code: a flexible method for

solution of the birth-death equations. *Atmospheric Chemistry and Physics* **2012,** *12*, (5), 2345-2355.
8. Myllys, N.; Chee, S.; Olenius, T.; Lawler, M.; Smith, J. J. T. J. o. P. C. A., Molecular-Level Understanding of Synergistic Effects in Sulfuric Acid–Amine–Ammonia Mixed Clusters. **2019,** *123*, (12), 2420-2425.
9. Chan, T. W.; Mozurkewich, M. J. J. o. a. s., Measurement of the coagulation rate constant for sulfuric acid particles as a function of particle size using tandem differential mobility analysis. **2001,** *32*, (3), 321-339.
10. Kürten, A.; Li, C.; Bianchi, F.; Curtius, J.; Dias, A.; Donahue, N. M.; Duplissy, J.; Flagan, R. C.; Hakala, J.; Jokinen, T.; Kirkby, J.; Kulmala, M.; Laaksonen, A.; Lehtipalo, K.; Makhmutov, V.; Onnela, A.; Rissanen, M. P.; Simon, M.; Sipilä, M.; Stozhkov, Y.; Tröstl, J.; Ye, P.; McMurry, P. H., New particle formation in the sulfuric acid–dimethylamine–water system: reevaluation of CLOUD chamber measurements and comparison to an aerosol nucleation and growth model. *Atmospheric Chemistry and Physics* **2018,** *18*, (2), 845-863.
11. Stolzenburg, D.; Simon, M.; Ranjithkumar, A.; Kürten, A.; Lehtipalo, K.; Gordon, H.; Nieminen, T.; Pichelstorfer, L.; He, X. C.; Brilke, S.; Xiao, M.; Amorim, A.; Baalbaki, R.; Baccarini, A.; Beck, L.; Bräkling, S.; Caudillo Murillo, L.; Chen, D.; Chu, B.; Dada, L.; Dias, A.; Dommen, J.; Duplissy, J.; El Haddad, I.; Finkenzeller, H.; Fischer, L.; Gonzalez Carracedo, L.; Heinritzi, M.; Kim, C.; Koenig, T. K.; Kong, W.; Lamkaddam, H.; Lee, C. P.; Leiminger, M.; Li, Z.; Makhmutov, V.; Manninen, H. E.; Marie, G.; Marten, R.; Müller, T.; Nie, W.; Partoll, E.; Petäjä, T.; Pfeifer, J.; Philippov, M.; Rissanen, M. P.; Rörup, B.; Schobesberger, S.; Schuchmann, S.; Shen, J.; Sipilä, M.; Steiner, G.; Stozhkov, Y.; Tauber, C.; Tham, Y. J.; Tomé, A.; Vazquez-Pufleau, M.; Wagner, A. C.; Wang, M.; Wang, Y.; Weber, S. K.; Wimmer, D.; Wlasits, P. J.; Wu, Y.; Ye, Q.; Zauner-Wieczorek, M.; Baltensperger, U.; Carslaw, K. S.; Curtius, J.; Donahue, N. M.; Flagan, R. C.; Hansel, A.; Kulmala, M.; Volkamer, R.; Kirkby, J.; Winkler, P. M., Enhanced growth rate of atmospheric particles from sulfuric acid. *Atmos. Chem. Phys. Discuss.* **2019,** *2019*, 1-17.
12. Hamaker, H. C., The London—van der Waals attraction between spherical particles. *Physica* **1937,** *4*, (10), 1058-1072.
13. Halonen, R.; Zapadinsky, E.; Kurtén, T.; Vehkamäki, H.; Reischl, B., Rate enhancement in collisions of sulfuric acid molecules due to long-range intermolecular forces. *Atmospheric Chemistry and Physics* **2019,** *19*, (21), 13355-13366.
14. Zheng, J.; Ma, Y.; Chen, M.; Zhang, Q.; Wang, L.; Khalizov, A. F.; Yao, L.; Wang, Z.; Wang, X.; Chen, L., Measurement of atmospheric amines and ammonia using the high resolution time-of-flight chemical ionization mass spectrometry. *Atmospheric Environment* **2015,** *102*, 249-259.
15. VandenBoer, T. C.; Petroff, A.; Markovic, M. Z.; Murphy, J. G., Size distribution of alkyl amines in continental particulate matter and their online detection in the gas and particle phase. *Atmospheric Chemistry and Physics* **2011,** *11*, (9), 4319-4332.
16. Ge, X.; Wexler, A. S.; Clegg, S. L., Atmospheric amines – Part I. A review. *Atmospheric Environment* **2011,** *45*, (3), 524-546.
17. Grönberg, L.; Lövkvist, P.; Jönsson, J. Å., Measurement of aliphatic amines in ambient air and rainwater. *Chemosphere* **1992,** *24*, (10), 1533-1540.
18. Hanson, D. R.; McMurry, P. H.; Jiang, J.; Tanner, D.; Huey, L. G., Ambient Pressure Proton Transfer Mass Spectrometry: Detection of Amines and Ammonia. *Environmental Science & Technology* **2011,** *45*, (20), 8881-8888.
19. Yu, H.; Lee, S.-H., Chemical ionisation mass spectrometry for the measurement of atmospheric amines. *Environmental Chemistry* **2012,** *9*, (3).
20. You, Y.; Kanawade, V. P.; de Gouw, J. A.; Guenther, A. B.; Madronich, S.; Sierra-Hernández, M. R.; Lawler, M.; Smith, J. N.; Takahama, S.; Ruggeri, G.; Koss, A.; Olson, K.; Baumann, K.; Weber, R. J.; Nenes, A.; Guo, H.; Edgerton, E. S.; Porcelli, L.; Brune, W. H.; Goldstein, A. H.; Lee, S. H., Atmospheric amines and ammonia measured with a chemical

ionization mass spectrometer (CIMS). *Atmospheric Chemistry and Physics* **2014,** *14*, (22), 12181-12194.
21. Cai, R.; Li, C.; He, X. C.; Deng, C.; Lu, Y.; Yin, R.; Yan, C.; Wang, L.; Jiang, J.; Kulmala, M.; Kangasluoma, J., Impacts of coagulation on the appearance time method for sub-3 nm particle growth rate evaluation and their corrections. *Atmos. Chem. Phys. Discuss.* **2020,** *2020*, 1-24.